BUILD SIMUL (2026) 19: 157–179
https://doi.org/10.1007/s12273-025-1371-2

Enhancing building resilience: Maintaining energy efficiency and thermal comfort during power outages in cold climates

Sang Hoon Lee[1] (✉), Carlo Bianchi[2], Juan Pablo Carvallo[1]

1. Lawrence Berkeley National Laboratory, Berkeley, CA 94720, USA
2. National Renewable Energy Laboratory, Boulder, CO 80401, USA

Research Article

Abstract

The increasing frequency and intensity of extreme weather events, such as heatwaves and cold snaps, present significant challenges to building energy performance and occupant comfort. Highly correlated with climate events are widespread long duration power interruptions that may affect thousands of buildings and millions of customers. This study evaluates the impact of building energy performance and occupant thermal comfort in medium-sized office buildings in a cold climate region. Using energy models representing pre-1980 and 2019 vintages, simulations were conducted to assess energy performance under typical weather conditions and occupant thermal comfort during power interrupted extreme cold snap and heatwave climate events under both current 2020s and future 2050s weather conditions. The results show a projected 33% increase in cooling energy demand and a 19% reduction in heating energy by 2050. Findings reveal that older buildings are more susceptible to cold discomfort during cold snaps, while modern airtight buildings are more vulnerable to overheating during heatwaves. Various passive energy efficiency measures, such as improved infiltration control, thermal windows, solar-controlled windows, and cool envelopes, were evaluated for their ability to mitigate thermal discomforts. Solar controlled windows and weatherstripping contribute to reducing cold thermal discomfort by 21% during a power-interrupted cold snap. Solar-controlled windows were found to reduce hot thermal discomfort by 34% during a future power-interrupted heatwave. The study highlights the importance of targeted retrofitting strategies to enhance thermal resilience, especially during power outages, to ensure occupant safety and comfort during extreme climate events.

Keywords

heatwave
cold snap
climate mitigation
thermal comfort
passive measures

Article History

Received: 24 June 2025
Revised: 22 September 2025
Accepted: 08 October 2025

Indoor/Outdoor Airflow and Air Quality

1 Introduction

Global temperatures are projected to continue rising, with significant increases expected if greenhouse gas emissions are not drastically reduced. Even with aggressive mitigation efforts, some level of warming is inevitable due to existing emissions (IPCC 2023). In the face of escalating extreme weather conditions, the resilience of buildings to such events has become a critical area of study. Extreme climate events, such as heatwaves and cold snaps, are projected to increase in frequency and severity, posing significant challenges to building performance and occupant comfort (Villa et al. 2022; Villa et al. 2024). While the overall frequency of cold snaps may decrease in a warming world, the intensity of individual cold events could remain high or even increase due to the disruptions in atmospheric patterns (Doss-Gollin et al. 2021). Conventional building designs may not be adequate to handle these extreme conditions, leading to discomfort, increased energy consumption, and potential health risks for occupants. Developing comprehensive strategies to enhance the thermal comfort and energy efficiency of buildings in the context of a warming climate is essential (Vijayan et al. 2022).

With rising temperatures contributing to an increase in the frequency and severity of extreme heatwaves and cold snaps, there is a growing focus on enhancing the thermal safety and resilience of buildings (Hinge 2023). Occupants' thermal safety in buildings during extreme climate events

E-mail: sanghlee@lbl.gov

refers to the ability of a building to maintain safe and comfortable indoor temperatures, protecting its inhabitants from the adverse effects of extreme heat or cold and ensuring activities developed in the building remain productive and effective. Ensuring thermal safety involves a combination of design, construction, and operational strategies to mitigate the risks associated with temperature extremes (Wagner et al. 2018). This focus is crucial as thermal safety directly impacts the health and comfort of building occupants (Sheng et al. 2023). Resilience refers to the ability of a building to recover from and adapt to adverse events (Field et al. 2012), and it serves as the foundation that enables thermal safety by helping buildings maintain safe indoor conditions during extreme temperature events. Resilient building design strategies help to mitigate risks. For instance, passive measures including insulation, solar-controlled windows, exterior coatings, and adaptive ventilation strategies contribute to maintaining a thermally safe indoor environment. A growing body of research has been dedicated to exploring the thermal resilience of buildings in the face of extreme climate events and future environmental changes. Hong et al. (2023b) conducted a broad review of the literature, identifying key questions and emphasizing the critical role of thermal resilience in a warming world. Siu et al. (2023) analyzed current methods for quantifying thermal resilience and explored how these methods could be integrated into building regulations and performance standards. Homaei and Hamdy (2021) proposed evaluation metrics to assess thermal performance during power outages. Benefits of thermal resilience beyond just energy efficiency were explored by advocating for policies and incentive programs that factor in occupant safety (Samuelson et al. 2020; Green-Mignacca et al. 2024). Siu et al. (2024) demonstrated automated evaluation of thermal resilience evaluation leveraging building energy models. On a global scale, initiatives such as the International Energy Agency's Annex 80 project on Resilient Cooling of Buildings are working to promote low-carbon, energy-efficient strategies for managing overheating risks (IEA 2023).

The aforementioned studies focus on blue sky conditions, in which weather events have not triggered loss of key building energy sources. Research indicates that extreme climate events increase the frequency of power outages, thereby compromising thermal safety for building occupants (Stone et al. 2021; Liang et al. 2025). Recent research has focused on assessing thermal comfort and resilience during power-interrupted heatwave events, as well as identifying strategies to mitigate occupants' thermal safety risks associated with climate extremes (Attia et al. 2021; Al-Assaad et al. 2025). A study investigated the thermal safety of occupants in an assisted living facility during a three-day winter storm in a hot-climate region, which coincided with widespread power outages (Sheng et al. 2023). In this work, we especially focus on the resilience response of an office building in a cold climate region under extreme weather events not only heatwaves but also cold snaps that trigger long duration power interruptions. Buildings cannot rely solely on active energy systems during power interruptions, making passive strategies essential (Zhang et al. 2021; Ismail et al. 2023). The use of passive strategies is effective in improving the thermal safety of occupants in buildings. Passive energy efficiency measures (EEMs) such as infiltration control, thermal windows, cool envelopes, and window coatings are effective in enhancing thermal comfort in buildings during extreme weather conditions (Yoon et al. 2021; Lee et al. 2024). High-performance building envelopes and solar-responsive design, contribute to thermal safety during power outages by maintaining habitable indoor conditions without relying on mechanical systems (Hachem-Vermette and Yadav 2023). These strategies aim to mitigate the adverse effects of extreme weather by reducing heat gain and loss, thereby enhancing the overall resilience of buildings (Holzer et al. 2024). Passive strategies enhance energy efficiency, reduce reliance on active systems, improve thermal comfort, and ensure greater resilience during power outages or extreme weather events (Erba and Barbieri 2022).

While research has primarily focused on enhancing thermal resilience and ensuring occupant thermal safety under extreme heat conditions in hot climate regions, this study shifts attention to cold climates. It investigates building energy performance and occupant thermal safety in the context of future extreme climate events, specifically in cold climate locations, and examines how passive energy efficiency measures (EEMs) can improve energy performance. Furthermore, the study explores the future evolution of both hot and cold extreme climate events in these regions and evaluates the potential of passive EEMs to enhance thermal safety for occupants during such extremes. While previous research has predominantly focused on thermal comfort under uninterrupted building operation, this study emphasizes occupants' thermal safety during both cold and hot extreme events under power outage conditions. The study uses current and future weather data to simulate the impact of future climate scenarios on office building performance in a cold climate location. Building energy simulations allow for a comprehensive analysis of how passive EEMs can contribute to maintaining thermal comfort and reducing energy efficiency in the context of evolving climate conditions. By focusing on both pre-1980 and 2019 vintage office buildings, this paper provides insights into the effectiveness of these measures across construction standards. In contrast to previous work, this study focuses on the thermal safety of intra-building spaces, identifying locational strategies that occupants could employ to improve their thermal comfort by relocating within a building space. The findings aim to inform building design and retrofitting practices, promoting thermally safer spaces in buildings capable of withstanding the challenges posed by extreme weather events.

2 Methods

The study aimed to analyze the energy performance of a medium office building in a cold climate region under typical recent and future weather conditions without power interruption and to evaluate occupants' thermal comfort during power interruptions caused by extreme climate. For the evaluation of energy and thermal comfort, the study used building energy models simulated using recent and future weather data. Grand Forks International Airport, located in North Dakota, USA, was selected as the representative cold-climate site for this study. According to ASHRAE Standard 169, it falls within Climate Zone 7, which characterizes regions with very cold weather conditions (ASHRAE 2020). This location was used to evaluate building energy performance and thermal comfort under extreme cold climate scenarios. Figure 1 shows the workflow of the building modeling and simulation process to evaluate occupants' thermal habitability.

2.1 Building energy model development

Building energy simulation is used to understand and illustrate how the energy performance and thermal comfort

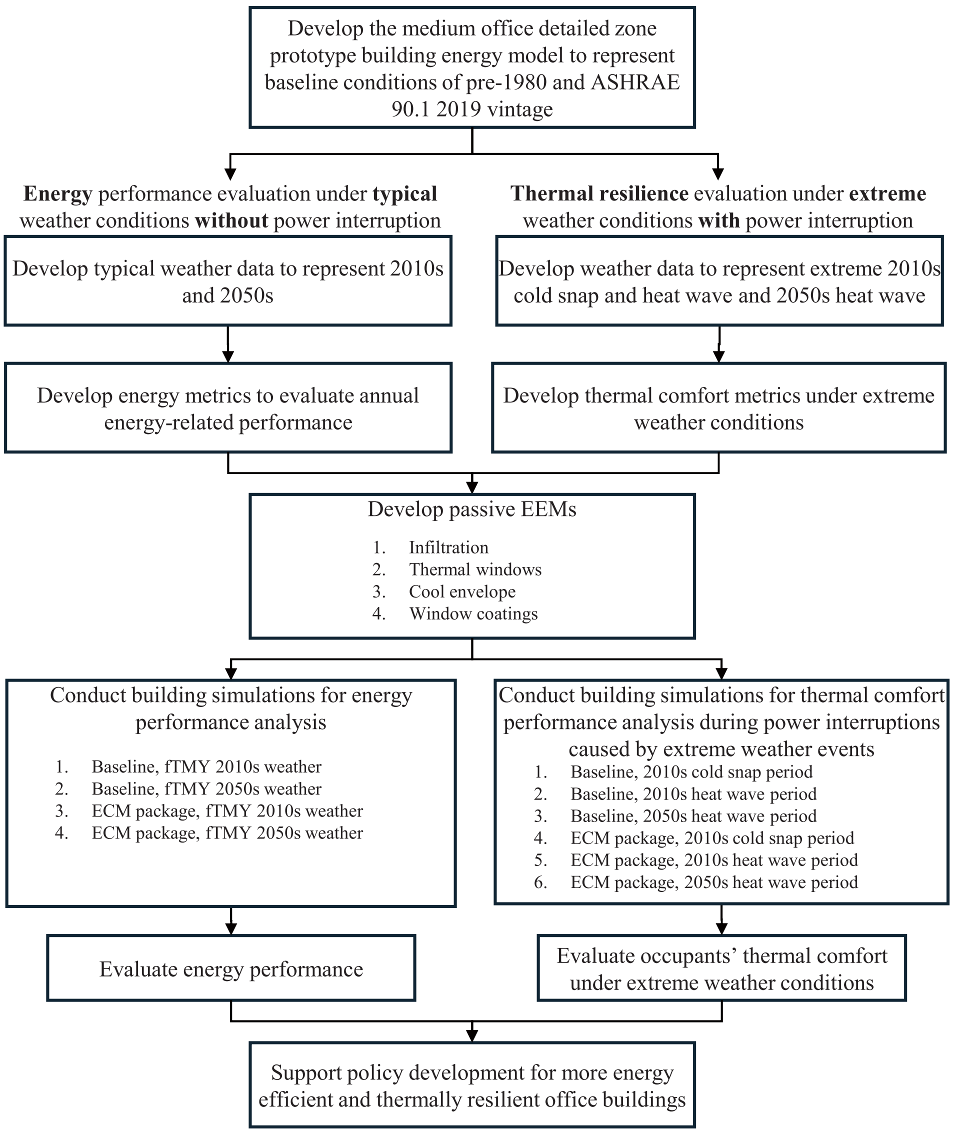

Fig. 1 Workflow to evaluate energy and thermal resilience performance for medium office buildings in recent and future weather conditions

metric vary due to different climate scenarios and building characteristics (Mathew et al. 2021). We used the U.S. Department of Energy (DOE) medium office prototype model that represents the pre-1980 vintage and ASHRAE 90.1-2019 compliant office buildings (Goel et al. 2014). Both vintage office building have steel-framed construction. The newer vintage incorporates improved thermal performance through increased insulation levels and reduced air leakage across the building envelope. The building envelope characteristics for the two vintages—Pre-1980 and ASHRAE 90.1-2019—are summarized as follows. The roof assembly thermal resistance is improved in the newer vintage, increasing from 2.80 $m^2 \cdot K/W$ in the pre-1980 model to 6.13 $m^2 \cdot K/W$ in the 2019 model. The exterior wall assembly thermal resistance increases from 1.15 $m^2 \cdot K/W$ to 3.45 $m^2 \cdot K/W$. Window performance also improves, with the thermal transmittance (U-value) decreasing from 3.53 $W/(m^2 \cdot K)$ in the older vintage to 1.66 $W/(m^2 \cdot K)$ in the 2019 standard. Additionally, the infiltration rate through the building envelope is reduced by nearly half, from 0.00113 $m^3/(s \cdot m^2)$ in the pre-1980 model to 0.00057 $m^3/(s \cdot m^2)$ in the ASHRAE 90.1-2019 model, reflecting improved air sealing practices in more recent construction. Each model is equipped with floor-level air handling units that provide natural gas-based space heating and direct expansion (DX) cooling, along with electric reheat for individual zone control. Both models assume a heating system efficiency of 0.80 and a cooling system coefficient of performance (COP) of 3.0. The heating setpoint is maintained at 21 °C during occupied hours and reduced to 15.6 °C during unoccupied periods. Cooling is set to 24 °C during occupied hours and 26.7 °C when unoccupied. Mechanical ventilation is provided throughout the building, while natural ventilation is not permitted.

We focus on office buildings because they are relatively large, typically occupied during many hours of the day, and prevalent in most cultures. The prototype medium office building used in this study is based on standardized datasets developed by the U.S. Department of Energy (DOE). These models are designed to reflect common building layouts and usage patterns across various space types. Figure 2 illustrates the 3D geometry of the medium office as modeled in EnergyPlus and visualized through the OpenStudio interface. Floor layouts for the top, middle, and bottom levels are shown in Figure 3. The building spans three stories, covers a total floor area of 4,980 m^2, and features a rectangular footprint with an aspect ratio of 1.5.

A detailed thermal zoning version of the model was used to improve realism compared to the default DOE prototype, which typically assigns only five zones per floor (Im et al. 2019). This refined version is available within the OpenStudio energy modeling environment (NREL 2024).

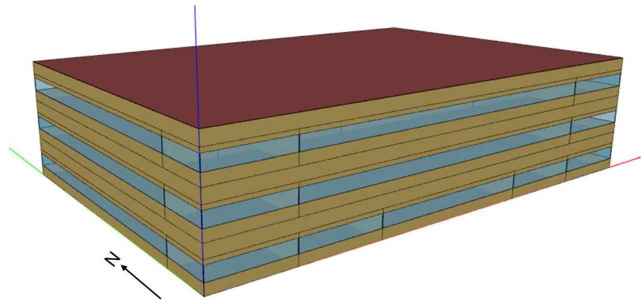

Fig. 2 Medium office detailed zone model 3D geometry

Utilizing these ready-to-use prototypes significantly reduces the time required to create custom models for each building, making large-scale simulation studies more feasible. The pre-1980 version of the office prototype represents older, less efficient buildings, while the 2019 version reflects compliance with the latest energy codes and standards.

2.2 Weather data

2.2.1 Future Typical Meteorological Year (fTMY) weather data

Future Typical Meteorological Year (fTMY) datasets condense multi-year climate projections into a single, representative weather year that reflects anticipated future conditions. These datasets are built upon outputs from global climate models, which simulate how the climate is expected to evolve over time (Chowdhury et al. 2024). Although climate models can generate weather data for individual years, relying on just one year may introduce biases due to atypical conditions. To address this, the Department of Energy applies the Typical Meteorological Year (TMY) methodology, which assembles a composite year by selecting statistically representative months across several years (Wilcox and Marion 2008). The same approach is extended to create fTMY data, where representative months are selected from projected future years generated by climate models. These projections are based on the IPCC's Shared Socio-economic Pathways (SSPs) and Representative Concentration Pathways (RCPs), collectively known as SSP-RCP scenarios (IPCC 2023). For this study, fTMY data aligned with the SSP5-RCP8.5 scenario were used. The resulting datasets are formatted as EnergyPlus Weather (EPW) files, enabling their direct application in building energy simulations to evaluate the impacts of climate change on building performance. It is important to recognize that while fTMY files provide a useful approximation of future climate averages, they do not account for extreme weather variability or the potential severity of future climate events (Chowdhury et al. 2024).

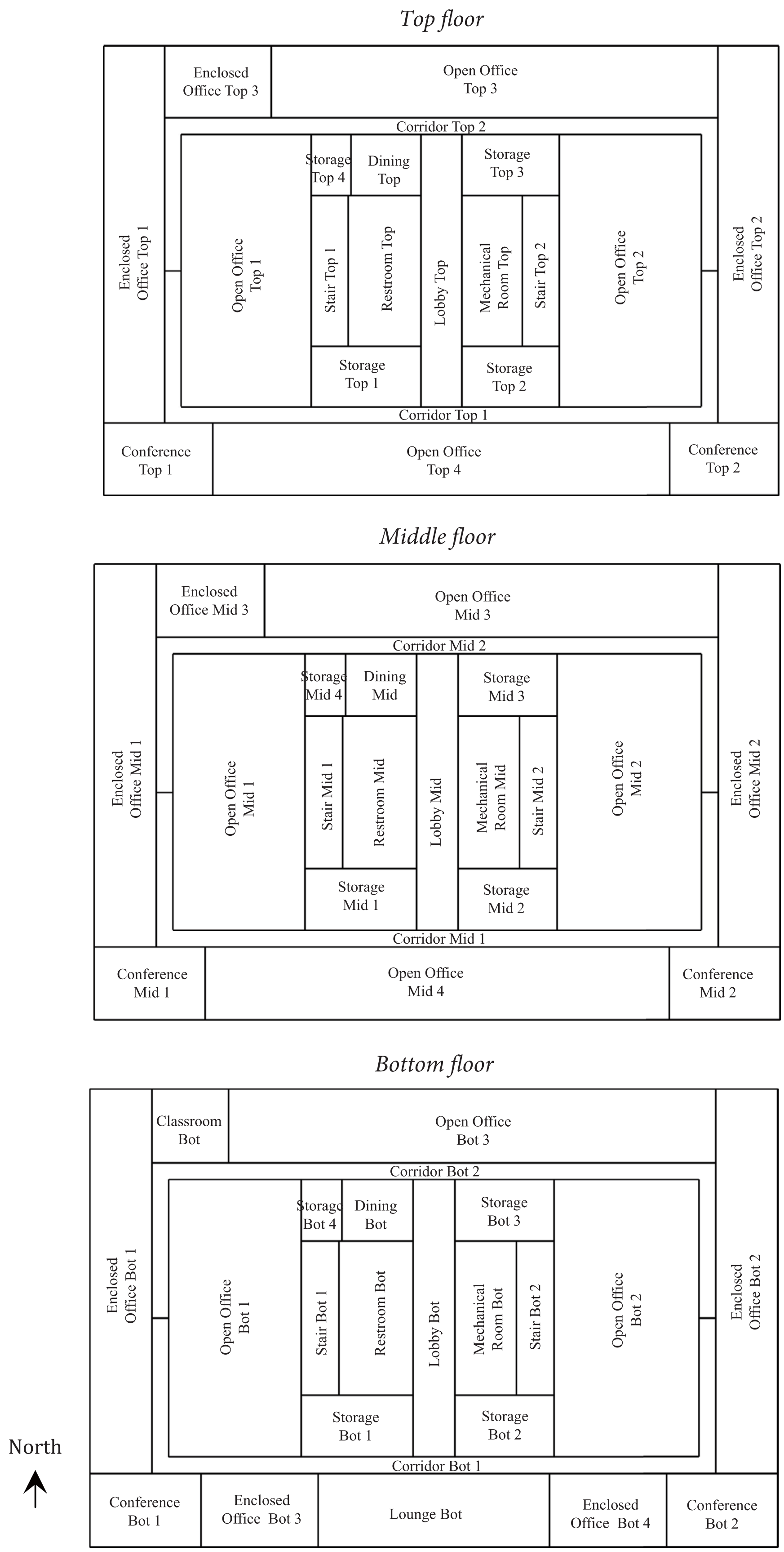

Fig. 3 Floor plans of top: top floor, middle: middle floor, and bottom: bottom floor for the medium office prototype model

2.2.2 Extreme climate events

To identify future extreme climate events, this study employed an hourly weather dataset derived from a regional climate model (RCM) (Zeng et al. 2023). A statistical approach based on upper and lower quantiles of daily air temperature was utilized to detect significant events such as heatwaves and cold snaps (Ouzeau et al. 2016). This method is versatile and can be applied globally, as it relies on relative temperature thresholds rather than fixed values. For heatwave detection, the 99.5th percentile (Spic_heatwave) of historical daily temperatures was used to identify peak intensity, while the 97.5th percentile (Sdeb_heatwave) served to assess both the duration (number of days above this threshold) and severity (expressed in °C·days). A heatwave was considered to end if temperatures fell below this level for more than three consecutive days, or below the 95th percentile (Sint_heatwave). Cold snaps were identified using the 0.5th percentile (Spic_coldsnap) as the indicator of extreme low temperatures, and the 2.5th percentile (Sdeb_coldsnap) for evaluating duration and severity, ending when temperatures exceeded the 5th percentile (Sint_coldsnap). For the selected cold-climate location of Grand Forks, the threshold temperature values were determined based on the percentile distribution of daily mean temperatures, as follows:

- Spic_heatwave: 26.9 °C, Sdeb_heatwave: 24.8 °C, Sint_heatwave: 23.5 °C;
- Spic_coldsnap: −26.6 °C, Sdeb_coldsnap: −23.0 °C, Sint_coldsnap: −19.8 °C.

This methodology has proven highly effective for evaluating heatwaves in building resilience research (Flores-Larsen et al. 2022) and was employed here to construct both typical and extreme weather profiles to assess building performance under climate stress—especially during heatwaves (Machard et al. 2024). Using this approach, multiple heatwave and cold snap events were identified for each selected multi-year period. For the resilience-focused thermal comfort analysis, the most intense instances of heatwaves and cold snaps were chosen as representative stress events.

The historical weather dataset, representing the ten-year period from 2014 to 2023, was obtained from the Modern-Era Retrospective Analysis for Research and Applications, version 2 (MERRA-2) and Global Hourly - Integrated Surface Database from the National Centers for Environmental Information, part of the U.S. National Oceanic and Atmospheric Administration weather data archive (Gelaro et al. 2017; NOAA National Centers for Environmental Information 2025). The future weather dataset, representing the ten-year period from 2045 to 2054, was derived from the projected climate dataset developed by Zeng et al. (2023). These ten-year historical and future weather data were used to detect extreme climate event. The most severe cold snap was detected in 2023 as shown in Table 1. As temperatures rise in the future, cold snaps were not detected from the future weather data from 2045 and 2054 based on the base 0.5 percentile temperature of the recent ten years of the weather data. On the other hand, future heatwaves become more severe. Table 2 shows the most severe heatwaves in the recent ten years and the future ten years between 2045 and 2054. The duration of the future heatwave is longer, and the severity and maximum daily mean temperature are greater than the heatwave from recent years.

2.3 Metrics to evaluate thermal comfort performance

For the occupant's thermal comfort analysis, clothing insulation was modeled dynamically, with values determined as a function of outdoor air temperature (DOE 2023). The occupants' metabolic rate was set to 120 W/person, representing typical office activity, and an air velocity of 0.2 m/s was applied in the thermal comfort analysis. Several metrics have been used to evaluate thermal comfort performance in buildings. The aggregate use of these metrics provides a comprehensive view of building thermal performance. We provide an overview of the metrics used in our study in Table 3 and their details as follows.

2.3.1 Predicted mean vote and predicted percentage discomfort

The predicted mean vote (PMV) index is used to assess the

Table 1 The most severe cold snap in recent (2014–2023) years and climate specifications

Cold snap	Begin	End	Duration (days)	Severity (°C·days)	Minimum daily mean temperature (°C)
Recent severe	2/6/2023	2/15/2023	10	7.4	−29.0

Table 2 The most severe heatwaves in the recent (2014–2023) and future (2045–2054) years and climate specifications

Heatwave	Begin	End	Duration (days)	Severity (°C·days)	Maximum daily mean temperature (°C)
Recent severe	8/15/2023	8/19/2023	5	5.7	28.7
Future severe	7/30/2054	8/13/2054	15	33.7	35.0

Table 3 Summary of thermal comfort evaluation metrics used in the study

Metric	Purpose	Discomfort thresholds	Applicable conditions
PMV/PPD	Quantifies perceived thermal sensation and discomfort based on heat balance	PMV < −2 (cold), PMV > +2 (hot)	Cold snaps and heatwaves
SET (standard effective temperature)	Measures heat stress based on equivalent temperature at 50% relative humidity	< 12 °C (cold), > 30 °C (hot)	Cold snaps and heatwaves
Adaptive comfort model	Evaluates comfort in naturally ventilated buildings based on operative temperature	Below/above ISO Category III adaptive temperature limits	Cold snaps and heatwaves
Hours of safety	Estimates duration before indoor temperatures drop below safe thresholds during outages	< 15.6 °C (mild), < 10 °C (moderate), < 4.4 °C (severe cold stress)	Cold snaps only
Heat index	Combines temperature and humidity to evaluate heat stress	> 26.7 °C (caution), > 32.2 °C (extreme caution), > 39.4 °C (Danger)	Heatwaves only
Integrated comfort rating	Aggregates normalized discomfort from all metrics to rank spaces	Based on normalized PPD, SET, adaptive model, safety (cold) or heat index (hot) discomfort hours	Space-level comparison under extremes

thermal comfort experienced by occupants. It represents the average thermal sensation vote on a scale from −3 (cold) to +3 (hot) based on responses from a large group of individuals (ASHRAE 2017). ISO Standards 17772-1 (ISO 2017) and 17772-2 (ISO 2018) incorporate the PMV–predicted percentage of dissatisfied (PPD) model for evaluating indoor thermal conditions. While the PMV–PPD model is typically applied to buildings equipped with mechanical heating and cooling, the adaptive model is better suited for naturally ventilated structures (ISO 2005). Building energy simulations are used to generate PMV values, incorporating weather data, building operation profiles, and occupant-specific parameters such as clothing and activity levels. Environmental inputs for PMV include air temperature, mean radiant temperature, air velocity, and humidity. Personal variables include clothing insulation and metabolic rate. For a realistic representation, clothing insulation levels are calculated using the dynamic predictive model from ASHRAE 55-2017, which adjusts based on outdoor air temperature (Lee and Schiavon 2014; ASHRAE 2017). The activity level is assumed to be 1.1 MET, typical for office work, corresponding to 65 W/m^2 (ASHRAE 2017). Hourly PMV values are analyzed for each thermal zone during power outage periods under extreme climate events. According to ASHRAE 55:2017, a PMV below −2 indicates significant cold discomfort, while values above +2 indicate extreme heat discomfort. To evaluate thermal discomfort, PPD-weighted exceedance hours are used. For cold conditions, these are calculated by summing the ratio of the actual PPD to the PPD at PMV = −2 whenever PMV drops below −2. Similarly, for heat, the ratio of actual PPD to the PPD at PMV = +2 is summed when PMV exceeds +2. These calculations follow the approach outlined in Annex H, Method C of ISO 17772-2:2018 (ISO 2018).

2.3.2 *Standard effective temperature*

This study uses the Standard Effective Temperature (SET), as outlined in ASHRAE 55-2017 (ASHRAE 2017), to assess the human physiological response to thermal stress (Zhang et al. 2023). SET represents the dry-bulb temperature of an isothermal space at 50% relative humidity where a person—wearing clothing appropriate for a specific activity—would experience the same level of skin temperature and moisture as in the actual environment. Threshold values of 30 °C for heat and 12 °C for cold are applied to evaluate thermal risk during extreme weather events (Lee and Levinson 2023; USGBC 2024). To quantify these risks, we calculate SET-based degree-weighted exceedance hours (°C·h): for heat stress, it is the total of (SET − 30 °C) during occupied hours when SET exceeds 30 °C; for cold stress, it is the total of (12 °C − SET) when SET is below 12 °C. However, because the duration of heatwaves and cold snaps varies by year, cumulative SET exceedance hours across entire events may not always provide a consistent basis for comparison.

2.3.3 *Adaptive model thermal comfort*

The adaptive comfort model is intended for “free-running” buildings—those without active heating or cooling systems. It presumes that occupants are generally inactive, and that thermal regulation is primarily achieved through natural ventilation, such as opening and closing windows. This approach is suitable for spaces where people have direct control over window operation and can adjust their clothing in response to indoor and outdoor conditions. The model assesses comfort based on operative temperature, which is typically calculated as the average of the air temperature and mean radiant temperature. According to ISO 17772-1:2017 Annex H.2 Category III, if the operative temperature exceeds the upper comfort limit based on the running mean of outdoor temperatures, the condition is classified as heat discomfort (ISO 2017). Conversely, if the operative temperature drops below the lower comfort threshold, it is considered cold discomfort. To quantify these deviations, we report degree-weighted exceedance hours: for heat, this is the cumulative sum of (operative temperature – upper limit) when positive during occupied hours, and for cold, it is the sum of (lower limit – operative temperature) when positive during the same period. It is important to note that the adaptive thermal comfort model requires the running mean outdoor air temperature to fall within the range of 10 °C to 30 °C for valid application. However, during the selected ten-day cold snap period, the running mean temperatures remained below the lower threshold, due to the extreme weather conditions characteristic of the cold-climate location. While the conditions do not strictly satisfy the applicability criteria of the adaptive model, this study demonstrates a methodological approach for evaluating thermal safety under extreme climate events. Despite these limitations, the analysis offers valuable insights into thermal resilience during periods of abnormal cold.

2.3.4 Hours of safety

The "hours of safety" concept provides a framework for estimating how long indoor environments can remain within safe temperature limits before becoming uncomfortably or dangerously cold, especially during power outages. This is particularly critical for assessing risks to vulnerable populations as severe cold weather events become more common. The framework assesses a building's ability to passively maintain habitable conditions based on its thermal properties and energy efficiency. It helps estimate how long occupants might be exposed to indoor temperatures that fall below health-related thresholds. For healthy individuals, thresholds are defined as follows: mild cold stress begins at 15.6 °C, moderate cold stress at 10 °C, and severe cold stress at 4.4 °C (Ayyagari et al. 2020). To evaluate exposure, we use a metric called "cold stress degree-weighted hours" (°C·h), calculated as the total of (15.6 °C minus the mean indoor dry-bulb temperature) during occupied hours, summing only the values above zero.

2.3.5 Heat index

The heat index is a metric that integrates both air temperature and relative humidity to reflect how hot it actually feels to the human body. Recognized by the U.S. Occupational Safety and Health Administration (OSHA) as a measure of heat stress (Kiersma 2014), it plays a crucial role in evaluating thermal comfort. The heat index values used here were derived from a regression formula developed by Lans P. Rothfusz (Steadman 1979). This index is particularly important because the body relies on sweating to maintain a stable internal temperature. However, when humidity is high, sweat evaporates more slowly, making it harder for the body to cool down and leading to a higher perceived temperature. Conversely, when humidity is low, sweat evaporates more efficiently, allowing the body to cool more effectively and feel cooler. The heat index is an indicator that combines both temperature and humidity and is widely used as an index to measure the comfort level felt by humans. It is considered as an indicator to assess heat stress by the Occupational Safety and Health Administration in the USA (Hong et al. 2023a). This index plays a key role in assessing human thermal comfort. When the body temperature rises, the body initiates sweating as a cooling mechanism. However, this natural process becomes less effective when evaporation is hindered—particularly in environments with high relative humidity. Under such humid conditions, sweat evaporates more slowly, reducing the body's ability to cool itself and making it feel hotter. In contrast, lower humidity levels enhance evaporation, which improves the body's cooling efficiency and makes the air feel cooler.

- Caution (26.7–32.2 °C): extended exposure to this range may lead to fatigue among building occupants. Extended physical activity could also result in heat cramps.
- Extreme caution (32.2–39.4 °C): this range presents a higher risk of heat-related illnesses. Activities carried out during this period may cause heat cramps, heat exhaustion, or potentially even heat stroke.
- Danger (39.4–51.7 °C): at these levels, the likelihood of heat cramps and heat exhaustion is high, and continuing activity may lead to heat stroke.

We report the heat index caution degree-weighted hours (°C·h), the sum of positive values of (26.7 °C minus mean heat index) during the occupied hours.

2.3.6 Integrated thermal comfort rating

We evaluated the thermal comfort for the working spaces during working hours using the introduced metrics. Figure 3 illustrates the floor plans of the prototype medium office building energy model. There are 65 spaces in total, and we selected 28 spaces directly related to the office type work. The selected space types are open office, closed office, conference room, and classroom in the bottom, middle, and top floor. We evaluated hot and cold thermal comfort for the selected working spaces during ten working hours from 8 a.m. to 6 p.m. We used the PMV–PPD-based thermal sensational scale, standard effective temperature, adaptive comfort model, thermal safety, and heat index thermal comfort metrics. We calculated the weighted hot and cold discomfort hours from the simulation results, and weighted discomfort hours are PPD-weighted hours from PMV–PPD thermal comfort and degree hours (°C·h) for SET, adaptive model, hours of safety, and heat index thermal comfort metrics. The weighted hot discomfort hours were used for the heatwave periods for the recent 2023 and future 2054 extreme heatwave events, and the weighted cold discomfort hours were used for the 2023 recent severe cold snap event. We assumed the power from the grid was disrupted during the extreme climate event to evaluate occupants' thermal comfort without active HVAC system support. As the heatwave and cold snap durations vary for the recent severe and future severe periods, the normalized metric to heatwave and cold snap duration was used to compare outcomes from extreme climate events of varying lengths.

1) Space-level cold discomfort rating

We evaluated the cold thermal comfort for the introduced metrics using the threshold of PMV < −2, SET < 12 °C, operative temperature below the adaptive model category three lower limit, and indoor dry-bulb air temperature below 15.6 °C from safety hours using mild cold stress. The integrated cold discomfort rating at a space level was developed to assess the combined impact of multiple thermal comfort indicators, as defined in Equation (1).

$$\begin{aligned}&SpaceColdDiscomfortRating_i\\&=\mathrm{Mean}\left(\frac{PPDcw_i}{PPDcw_{\max}},\frac{SETcw_i}{SETcw_{\max}},\frac{OTcw_i}{OTcw_{\max}},\frac{SHcw_i}{SHcw_{\max}}\right)\end{aligned} \tag{1}$$

where, $PPDcw_i$ is the PPD cold weighted discomfort hours for space i; $PPDcw_{\max}$ is the maximum PPD cold weighted discomfort hours from all the working spaces; $SETcw_i$ is the standard effective temperature cold weighted discomfort hours for space i; $SETcw_{\max}$ is the maximum standard effective temperature cold weighted discomfort hours from all the working spaces; $OTcw_i$ is the adaptive model-based operative temperature cold weighted discomfort hours for space i; $OTcw_{\max}$ is the adaptive model-based maximum operative temperature cold weighted discomfort hours from all the working spaces; $SHcw_i$ is the safety hours-based indoor dry-bulb temperature cold weighted discomfort hours for space i; $SHcw_{\max}$ is the safety hours-based maximum dry-bulb temperature cold weighted discomfort hours from all the working spaces.

2) Space-level hot discomfort rating

We calculated the hot weighted discomfort hours using the threshold of PMV > +2, SET > 30 °C, operative temperature above the adaptive model category three upper limit, and heat index above the caution limit (26.7 °C) for each working space during the extreme heatwave events for the recent 2023 and future 2054 heatwave period. The integrated hot discomfort rating was formulated at a spatial level to assess the cumulative impact of multiple thermal comfort indicators, as defined in Equation (2).

$$\begin{aligned}&SpaceHotDiscomfortRating_i\\&=\mathrm{Mean}\left(\frac{PPDhw_i}{PPDhw_{\max}},\frac{SEThw_i}{SEThw_{\max}},\frac{OThw_i}{OThw_{\max}},\frac{HIhw_i}{HIhw_{\max}}\right)\end{aligned} \tag{2}$$

where, $PPDhw_i$ is the PPD hot weighted discomfort hours for space i; $PPDhw_{\max}$ is the maximum PPD hot weighted discomfort hours from all the working spaces; $SEThw_i$ is the standard effective temperature hot weighted discomfort hours for space i; $SEThw_{\max}$ is the maximum standard effective temperature hot weighted discomfort hours from all the working spaces; $OThw_i$ is the adaptive model-based operative temperature hot weighted discomfort hours for space i; $OThw_{\max}$ is the adaptive model-based maximum operative temperature hot weighted discomfort hours from all the working spaces; $HIhw_i$ is the heat index caution weighted discomfort hours for space i; $HIhw_{\max}$ is the maximum heat index caution weighted discomfort hours from all the working spaces.

Space-level discomfort rating is valid to compare the discomfort levels among spaces. These space-level thermal comfort ratings might be further extended for evaluation of the building-level thermal comfort evaluation adopting an area-weighted or occupants-weighted average of space-level metrics.

2.4 Energy conservation measure package

This study investigates four passive energy efficiency measures (EEMs) that improve thermal comfort in buildings subjected to extreme weather conditions. The EEMs examined include infiltration control, thermal windows, cool envelopes, and window coatings.

(1) Infiltration control: infiltration measures involve air sealing to reduce envelope leaks, achieving a 30% reduction in infiltration compared to baseline models.

(2) Thermal windows: this measure replaces single-pane glazing systems with double-pane glazing systems. For pre-1980 vintage office buildings, which originally have single-pane glazing with a thermal transmittance (U-value) of 3.52 W/(m^2·K), the upgrade to double-pane glazing systems with a U-value of 1.66 W/(m^2·K) complies with ASHRAE 90.1 2019 specifications. The 2019 vintage office buildings already feature double-pane windows, so no changes are necessary for this measure.

(3) Cool envelope strategy: the cool envelope strategy aims to reduce solar heat gain by enhancing the solar reflectance of the roof and walls. The prototype baseline office has a conventional gray roof and walls with a solar reflectance of 0.3. By applying bright-white paints, the solar reflectance is increased to 0.6.

(4) Window coatings: this measure involves applying a low solar heat gain coefficient (SHGC) film to windows. For pre-1980 office buildings, the SHGC is reduced from 0.41 to 0.15. For 2019 vintage buildings, the SHGC is reduced from 0.36 to 0.15.

3 Results and discussions

Results are reported in three subsections. First, we report the annual energy performance of buildings to highlight the performance differences across the two vintages explored in this work and for current and future weather conditions. Second, we report the response of both building vintages to cold snaps under a ten-day power interruption event for current weather conditions, with and without passive EEMs. Finally, we report the response of both building vintages to heatwaves under a 15-day power interruption event for future weather conditions, with and without passive EEMs. The scenario choice for extreme weather events covers the widest possible performance range and hence comprehensively analyzes the role of passive EEMs in improving building thermal safety under long duration power interruptions. A power interruption consequence no electricity service from the energy grid, which results in inoperable energy systems such as HVAC systems, portable heaters or cooling equipment, and ceiling fans—any equipment supported by the electrical plug load.

3.1 Annual energy performance

The ASHRAE 90.1 2019 code-compliant medium office building incorporates advanced energy-efficient technologies across the building energy systems. This results in significantly lower energy consumption compared to the pre-1980 vintage office building. Table 4 provides energy consumption by end-use type for both 2019 and pre-1980 vintage medium office buildings under 2020 and 2050 weather conditions. The 2019 baseline building demonstrates a reduction in electricity consumption by approximately 37% and natural gas consumption by about 49% compared to the pre-1980 baseline. These savings are attributed to more efficient HVAC systems, lighting, electric equipment, and improved thermal insulation technologies.

The medium office prototype model utilizes a heating system comprising a natural gas-based central boiler and an electric terminal reheat system, resulting in heating consumption from both natural gas and electricity. Figure 4 presents the heating and cooling performance changes due to future climate and the application of passive EEMs. For the comparison, we used source energy for electricity-based cooling and natural gas-based heating. A source energy factor of 2.5 for electricity and 1.09 for natural gas, based on the 2020 North Dakota state average, was applied to derive the source energy from electricity and natural gas usage (GTI Energy 2023). Given the very cold climate location of this prototype medium office building, the heating source energy consumption is significantly greater than the cooling source energy consumption. Under 2020 weather conditions, the pre-1980 office building's heating source energy is about 6.4 times greater than its cooling source energy, which changes to 3.9 times under 2050 weather conditions due to future climate. The 2019 code-compliant office shows a heating source energy consumption 2.8 times higher than cooling source energy in 2020, which changes

Table 4 2019 and pre-1980 vintage prototypical medium office energy performance in climate zone 7 under 2020 and 2050 weather conditions for the baseline and EEM scenarios

			Electricity (kWh/a)								Natural gas (kWh/a)		
Vintage	Weather	EEM	Heating	Cooling	Interior lighting	Exterior lighting	Plug load	Fans	Pumps	**Electricity total**	Heating	Water heating	**Natural gas total**
2019	2020	Baseline	84,079	66,570	85,353	29,092	201,766	13,757	41	**480,657**	235,324	27,182	**262,506**
2019	2020	Cool envelope	85,740	64,626	85,353	29,092	201,766	13,381	41	**479,997**	231,308	27,182	**258,490**
2019	2020	Infiltration	76,689	66,740	85,353	29,092	201,766	13,775	41	**473,456**	235,851	27,177	**263,028**
2019	2020	Solar-control window	95,290	52,524	85,353	29,092	201,766	10,965	41	**475,030**	199,295	27,182	**226,477**
2019	2020	Thermal window	84,079	66,570	85,353	29,092	201,766	13,757	41	**480,657**	235,324	27,182	**262,506**
2019	2050	Baseline	68,261	88,291	85,353	29,092	201,766	14,721	41	**487,524**	189,419	27,179	**216,598**
2019	2050	Cool envelope	69,131	87,065	85,353	29,092	201,766	14,506	41	**486,953**	187,690	27,178	**214,868**
2019	2050	Infiltration	62,405	88,493	85,353	29,092	201,766	14,758	41	**481,908**	189,819	27,177	**216,997**
2019	2050	Solar-control window	77,474	70,563	85,353	29,092	201,766	11,569	41	**475,858**	160,204	27,188	**187,392**
2019	2050	Thermal window	68,261	88,291	85,353	29,092	201,766	14,721	41	**487,524**	189,419	27,179	**216,598**
Pre-1980	2020	Baseline	477,611	109,726	309,061	77,600	280,876	28,863	127	**1,283,863**	510,481	25,990	**536,471**
Pre-1980	2020	Cool envelope	480,302	105,956	309,061	77,600	280,876	28,096	127	**1,282,018**	499,523	25,991	**525,515**
Pre-1980	2020	Infiltration	393,519	108,767	309,061	77,600	280,876	28,392	127	**1,198,342**	509,797	25,973	**535,771**
Pre-1980	2020	Solar-control window	484,240	93,471	309,061	77,600	280,876	25,078	127	**1,270,452**	453,656	26,000	**479,656**
Pre-1980	2020	Thermal window	390,349	110,046	309,061	77,600	280,876	28,723	127	**1,196,783**	511,814	25,977	**537,791**
Pre-1980	2050	Baseline	403,945	149,486	309,061	77,600	280,876	32,428	127	**1,253,523**	410,211	25,980	**436,191**
Pre-1980	2050	Cool envelope	406,481	144,760	309,061	77,600	280,876	31,527	127	**1,250,432**	401,363	25,982	**427,346**
Pre-1980	2050	Infiltration	330,591	148,000	309,061	77,600	280,876	31,944	127	**1,178,198**	409,855	25,967	**435,822**
Pre-1980	2050	Solar-control window	412,605	128,338	309,061	77,600	280,876	27,845	127	**1,236,452**	364,149	25,989	**390,138**
Pre-1980	2050	Thermal window	325,712	149,601	309,061	77,600	280,876	32,233	127	**1,175,210**	411,427	25,969	**437,396**

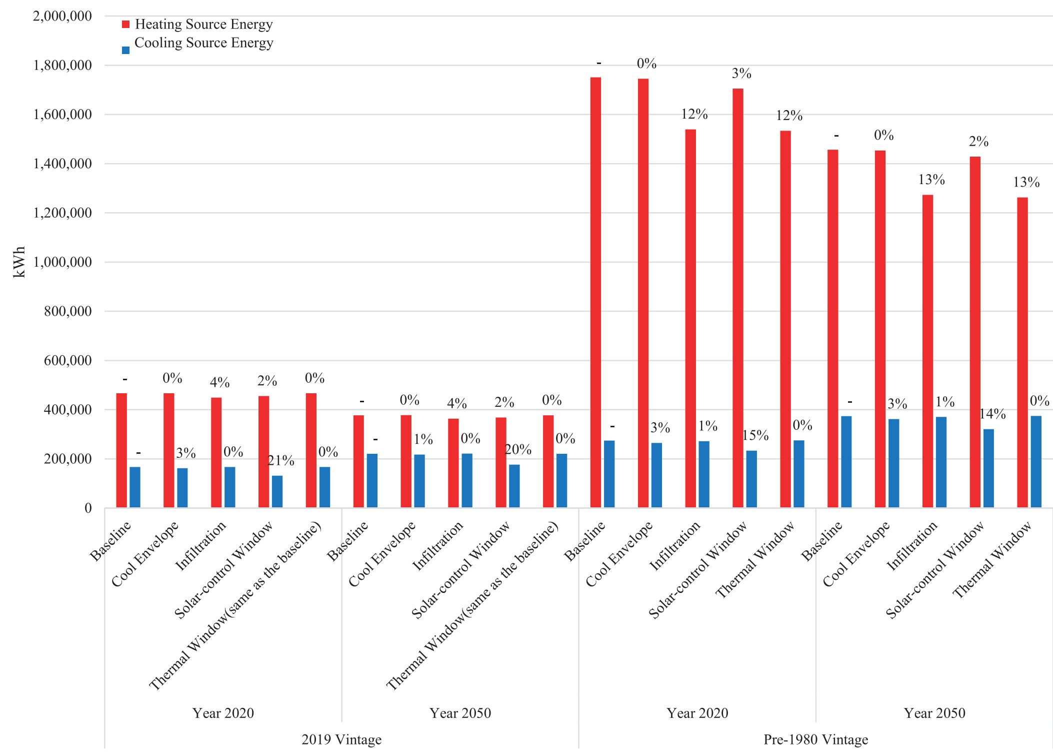

Fig. 4 Heating and cooling source energy performance changes in kWh and fractional reduction in percentage from future climate as well as passive energy conservation measure application for 2019 and pre-1980 vintage office building

to 1.7 times in 2050. Additionally, the office's reheat system with electricity leads to an observed electricity peak during winter morning hours.

2050 weather conditions result in a 33% increase in cooling energy consumption and a 19% decrease in heating energy consumption for the 2019 vintage baseline office building compared to 2020 weather conditions. The pre-1980 building exhibits a similar trend. When passive thermal resilient technologies are applied to the baseline building, improvements in airtightness to reduce infiltration airflow rate and the installation of low-*U*-value thermal windows can contribute to approximately 12% heating source energy reduction. The 2019 vintage office can benefit from about a 4% reduction in heating energy due to the infiltration measure. These infiltration and thermal window improvements yield similar heating source energy savings in both 2020 and 2050 weather conditions but have a minor effect on cooling energy performance changes. Given that the 2019 code-compliant building already features thermally insulated windows, further upgrades to window thermal performance were not analyzed.

On the other hand, solar-control window film can significantly reduce cooling energy consumption, contributing to about 20% savings for the 2019 office and 15% for the pre-1980 office (Figure 4). Additionally, the cool envelope strategy can achieve approximately 3% savings in cooling energy in both 2020 and 2050 weather conditions. These window films and cooling surfaces increase electric reheat energy but reduce central boiler natural gas heating energy, resulting in minor changes to overall heating source energy performance.

3.2 Thermal comfort performance under cold snap events

3.2.1 *Baseline condition*

The prototype office building, representing pre-1980 vintage structures, is significantly more vulnerable to cold thermal discomfort during a power-interrupted cold snap event compared to the 2019 office building. Consequently, our analysis focuses on cold thermal discomfort in the pre-1980 vintage office prototype. Table 5 provides a comprehensive analysis of the pre-1980 office's space-level thermal comfort over a ten-day period of power interruptions during a cold snap in 2023. The table includes the total number of hours, normalized by the cold snap duration, and weighted discomfort hours for each cold thermal comfort metric: PMV (predicted mean vote), SET (standard effective temperature), adaptive model, and safety hours. The analysis focuses on ten working hours between 8 a.m. and 6 p.m. during the cold snap.

Table 5 Cold thermal discomfort rating for each workable space for pre-1980 vintage baseline office during the 2023 cold snap with power outage

Vintage	Scenario	EEM	Space	Area [m²]	PMV<-2 hours [h/d]	PMV<-2 weighted discomfort hours [TSSU·h/d]	PMV cold rating	SET<12 cold stress hours [h/d]	SET<12 weighted cold stress hours [°C·h/d]	SET cold rating	Adaptive cold hours [h/d]	Adaptive weighted cold hours [°C·h/d]	Adaptive cold rating	Safety<16 cold hours [h/d]	Safety<16 weighted cold hours [°C·h/d]	Safety cold rating	**Integrated cold rating**
Pre1980	2023 Cold snap	Baseline	ENCLOSEDOFFICE_TOP_3	42	9	12	98%	7	14	100%	9	50	100%	10	113	100%	**99%**
			OPENOFFICE_TOP_3	176	9	12	98%	7	14	98%	9	50	99%	10	113	100%	**99%**
			ENCLOSEDOFFICE_TOP_1	126	9	12	100%	6	12	90%	9	48	95%	10	113	100%	**96%**
			ENCLOSEDOFFICE_TOP_2	126	9	12	99%	6	9	66%	8	43	87%	10	109	97%	**87%**
			ENCLOSEDOFFICE_BOT_1	126	9	11	96%	5	9	62%	9	42	83%	10	107	95%	**84%**
			OPENOFFICE_BOT_3	189	9	11	97%	6	8	59%	8	41	83%	10	104	92%	**83%**
			ENCLOSEDOFFICE_MID_1	126	9	11	95%	4	7	52%	8	37	73%	10	101	90%	**77%**
			ENCLOSEDOFFICE_BOT_2	126	9	11	97%	4	6	44%	8	38	76%	10	104	92%	**77%**
			ENCLOSEDOFFICE_MID_3	42	9	11	96%	4	6	47%	8	38	76%	10	100	89%	**77%**
			OPENOFFICE_MID_3	176	9	11	96%	4	6	45%	8	37	75%	10	100	88%	**76%**
			ENCLOSEDOFFICE_MID_2	126	9	11	96%	3	5	34%	8	32	65%	10	98	86%	**70%**
			CLASSROOM_BOT	30	8	10	86%	2	3	24%	8	25	50%	10	76	67%	**57%**
			OPENOFFICE_TOP_4	180	8	9	79%	2	2	15%	6	18	37%	10	73	65%	**49%**
			OPENOFFICE_TOP_1	194	7	8	70%	1	0	3%	6	18	36%	8	59	53%	**40%**
			OPENOFFICE_TOP_2	212	7	8	70%	1	0	3%	6	18	36%	8	59	52%	**40%**
			CONFROOM_TOP_1	43	6	7	61%	2	2	18%	4	15	29%	9	60	53%	**40%**
			CONFROOM_TOP_2	43	6	7	60%	1	2	15%	4	12	25%	9	58	51%	**38%**
			OPENOFFICE_MID_4	180	7	8	66%	1	1	6%	4	11	23%	9	60	53%	**37%**
			ENCLOSEDOFFICE_BOT_3	45	7	8	70%	1	0	3%	4	9	19%	10	60	53%	**36%**
			ENCLOSEDOFFICE_BOT_4	45	7	8	70%	1	0	3%	4	9	19%	10	60	53%	**36%**
			CONFROOM_BOT_1	43	5	6	54%	1	1	9%	3	10	21%	9	55	49%	**33%**
			CONFROOM_BOT_2	43	5	6	53%	1	1	8%	3	9	18%	9	53	47%	**31%**
			CONFROOM_MID_1	43	5	6	49%	1	1	10%	3	10	20%	9	51	45%	**31%**
			CONFROOM_MID_2	43	5	5	46%	1	1	8%	3	9	18%	9	48	43%	**29%**
			OPENOFFICE_MID_1	194	5	6	50%	-	-	0%	4	7	14%	8	41	37%	**25%**
			OPENOFFICE_MID_2	212	5	6	50%	-	-	0%	4	7	14%	8	41	36%	**25%**
			OPENOFFICE_BOT_1	194	1	1	9%	-	-	0%	1	1	1%	6	21	19%	**7%**
			OPENOFFICE_BOT_2	212	1	1	9%	-	-	0%	1	1	1%	6	21	19%	**7%**

The PMV and adaptive model metrics indicate that several office spaces experience nine hours of thermally cold conditions. The safety hours metric reveals that almost half of the workable spaces are unsafe from the cold for the entire working day. The SET metric shows that two office spaces endure seven hours of cold stress conditions.

Table 5 also provides a cold thermal performance rating for each space based on the weighted discomfort hours for each metric. The far-right column presents an integrated cold rating derived from Equation (1) developed specifically for this study. This integrated metric indicates that the northern top floor offices are the most vulnerable to cold thermal discomfort. Following closely are the offices on the top and bottom floors located in the east and west. The intra-building cold thermal performance evaluation reveals that perimeter zones on the top and bottom floors are the most vulnerable to cold conditions. Specifically, the top floor perimeter spaces are the poor performers, followed by the bottom and mid floors. South-facing offices with solar heat gains and inner zones without windows are safer during cold events. Conference and classroom spaces with higher occupant densities can offer better protection during cold snaps. Figure 5 illustrates the color-coded cold thermal discomfort rating in the top, mid, and bottom floor plans for the pre-1980 vintage office building under the power-interrupted extreme cold snap event in 2023

3.2.2 *Cold thermal comfort improvement with passive EEMs*

Table 6 presents the changes in cold thermal comfort resulting from retrofitting the building to reduce infiltration, thereby decreasing the airflow between the exterior and interior by 30% from the baseline condition. Table 7 illustrates the impact of upgrading the building's windows from baseline single-pane to double-pane, more thermally insulated windows. The discomfort-weighted hour rating is calculated based on the baseline worst space condition. Enhancing the airtightness of the building envelope to reduce unwanted airflow infiltration significantly improves cold thermal performance. The infiltration retrofit decreases the discomfort-weighted hours across all metrics: PMV, SET, adaptive model, and safety hours. Specifically, the worst-performing space, an enclosed office on the top north side, shows a 21% improvement in the integrated cold discomfort rating. Upgrading to double-pane, thermally insulated windows enhance the cold thermal comfort of the worst space by 17%. These EEMs are particularly beneficial for perimeter spaces, significantly improving thermal comfort compared to core zone open offices (Open Office 1 and 2) on all three floors.

Table 8 presents the building-level cold thermal performance rating, which integrates space-level ratings using an area-weighted average. The baseline condition shows a discomfort rating of 52%. Implementing the infiltration

Fig. 5 Color-coded cold thermal discomfort rating in the top, mid, and bottom floor plans for the pre-1980 vintage office building under power-interrupted extreme cold snap event in 2023

reduction measure improves the building-level weighted discomfort by 16%, while upgrading to thermal windows results in a 12% improvement. Although cool envelope and solar-control window measures are advantageous for reducing solar heat gain during the hot season, they have detrimental effects during cold snap periods. Specifically, the cool envelope measure worsens cold thermal comfort by 3%, and the solar-control window measure exacerbates it by 18%.

3.3 Thermal comfort performance under heatwave events

3.3.1 *Baseline condition*

The 2019 vintage office building may face more dangerous heat-related risks than the pre-1980 vintage office indoor thermal conditions in a power-interrupted severe hot climate environment. The latest building code is more air-tight and thermal insulated compared to the old vintage buildings.

Table 6 Cold thermal discomfort rating for each workable space for pre-1980 vintage office with infiltration measure during the 2023 cold snap with power outage

Vintage	Scenario	EEM	Space	Area [m²]	PMV<-2 hours [h/d]	PMV<-2 weighted discomfort hours [TSSU·h/d]	PMV cold rating	SET<12 cold stress hours [h/d]	SET<12 weighted cold stress hours [°C·h/d]	SET cold rating	Adaptive cold hours [h/d]	Adaptive weighted cold hours [°C·h/d]	Adaptive cold rating	Safety<16 cold hours [h/d]	Safety<16 weighted cold hours [°C·h/d]	Safety cold rating	**Integrated cold rating**
Pre1980	2023 Cold snap	Infiltration	ENCLOSEDOFFICE_TOP_3	42	9	11	96%	5	7	49%	8	39	77%	10	99	87%	**78%**
			OPENOFFICE_TOP_3	176	9	11	96%	5	7	48%	8	38	77%	10	99	87%	**77%**
			ENCLOSEDOFFICE_TOP_1	126	9	11	93%	4	7	49%	8	36	72%	10	98	87%	**75%**
			ENCLOSEDOFFICE_TOP_2	126	9	11	94%	3	4	30%	8	32	63%	10	94	83%	**68%**
			ENCLOSEDOFFICE_BOT_1	126	9	11	92%	3	3	25%	8	29	57%	10	90	80%	**63%**
			OPENOFFICE_BOT_3	189	8	11	89%	2	3	21%	7	29	58%	10	88	78%	**62%**
			ENCLOSEDOFFICE_BOT_2	126	8	11	90%	1	2	18%	7	25	51%	10	87	77%	**59%**
			ENCLOSEDOFFICE_MID_3	42	8	10	88%	1	3	19%	7	25	50%	10	83	74%	**58%**
			OPENOFFICE_MID_3	176	8	10	87%	1	3	19%	7	25	50%	10	83	74%	**57%**
			ENCLOSEDOFFICE_MID_1	126	8	10	88%	2	3	21%	7	23	47%	10	84	74%	**57%**
			ENCLOSEDOFFICE_MID_2	126	8	10	84%	1	2	16%	7	20	40%	10	80	70%	**52%**
			CLASSROOM_BOT	30	8	10	81%	1	2	11%	6	13	27%	9	60	53%	**43%**
			OPENOFFICE_TOP_4	180	7	8	66%	1	1	5%	4	11	21%	9	57	50%	**36%**
			OPENOFFICE_TOP_1	194	6	7	60%	-	-	0%	5	11	23%	8	51	45%	**32%**
			OPENOFFICE_TOP_2	212	6	7	60%	-	-	0%	5	11	23%	8	51	45%	**32%**
			CONFROOM_TOP_1	43	5	5	45%	1	1	7%	3	8	17%	9	43	38%	**27%**
			CONFROOM_TOP_2	43	4	4	36%	1	1	5%	2	7	14%	9	41	36%	**23%**
			OPENOFFICE_MID_4	180	4	5	42%	0	0	1%	2	5	10%	9	42	37%	**23%**
			ENCLOSEDOFFICE_BOT_3	45	4	5	40%	0	0	0%	2	4	7%	9	41	37%	**21%**
			ENCLOSEDOFFICE_BOT_4	45	4	5	40%	0	0	0%	2	4	7%	9	41	37%	**21%**
			CONFROOM_BOT_1	43	4	4	35%	0	0	2%	2	5	10%	8	36	32%	**20%**
			CONFROOM_MID_1	43	3	4	29%	0	0	3%	2	5	10%	7	33	29%	**18%**
			CONFROOM_BOT_2	43	3	4	31%	0	0	1%	2	4	9%	8	34	30%	**18%**
			OPENOFFICE_MID_1	194	4	4	34%	-	-	0%	2	2	4%	7	31	28%	**17%**
			OPENOFFICE_MID_2	212	4	4	32%	-	-	0%	2	2	4%	7	31	27%	**16%**
			CONFROOM_MID_2	43	2	3	24%	0	0	2%	2	4	9%	8	30	27%	**15%**
			OPENOFFICE_BOT_1	194	-	-	0%	-	-	0%	-	-	0%	5	14	12%	**3%**
			OPENOFFICE_BOT_2	212	-	-	0%	-	-	0%	-	-	0%	5	14	12%	**3%**

Table 7 Cold thermal discomfort rating for each workable space for pre-1980 vintage with thermal windows measure office during the 2023 cold snap with power outage

Vintage	Scenario	EEM	Space	Area [m²]	PMV<-2 hours [h/d]	PMV<-2 weighted discomfort hours [TSSU·h/d]	PMV cold rating	SET<12 cold stress hours [h/d]	SET<12 weighted cold stress hours [°C·h/d]	SET cold rating	Adaptive cold hours [h/d]	Adaptive weighted cold hours [°C·h/d]	Adaptive cold rating	Safety<16 cold hours [h/d]	Safety<16 weighted cold hours [°C·h/d]	Safety cold rating	**Integrated cold rating**
Pre1980	2023 Cold snap	Thermal Windows	ENCLOSEDOFFICE_TOP_3	43	9	11	97%	5	8	59%	8	41	83%	10	103	91%	**82%**
			OPENOFFICE_TOP_3	194	9	11	97%	5	8	58%	8	41	82%	10	103	91%	**82%**
			ENCLOSEDOFFICE_TOP_1	212	9	11	94%	5	8	57%	8	39	77%	10	103	91%	**80%**
			ENCLOSEDOFFICE_TOP_2	43	9	11	96%	3	5	36%	8	34	69%	10	99	88%	**72%**
			ENCLOSEDOFFICE_BOT_1	42	9	11	92%	3	4	32%	8	32	64%	10	97	86%	**69%**
			OPENOFFICE_BOT_3	45	8	11	90%	3	4	28%	8	32	65%	10	94	83%	**66%**
			ENCLOSEDOFFICE_BOT_2	176	9	11	92%	2	3	22%	8	29	58%	10	94	83%	**64%**
			ENCLOSEDOFFICE_MID_3	194	8	11	89%	2	3	25%	7	29	57%	10	89	79%	**63%**
			ENCLOSEDOFFICE_MID_1	30	8	10	88%	3	4	28%	8	27	54%	10	90	80%	**62%**
			OPENOFFICE_MID_3	43	8	11	89%	2	3	24%	7	28	57%	10	89	79%	**62%**
			ENCLOSEDOFFICE_MID_2	180	8	10	87%	1	3	20%	7	23	47%	10	87	77%	**58%**
			CLASSROOM_BOT	42	8	10	83%	1	2	14%	7	17	33%	9	66	58%	**47%**
			OPENOFFICE_TOP_4	212	7	8	68%	1	1	7%	5	13	25%	10	63	56%	**39%**
			OPENOFFICE_TOP_1	212	6	7	62%	-	-	0%	5	13	26%	8	53	47%	**34%**
			OPENOFFICE_TOP_2	43	6	7	62%	-	-	0%	5	13	26%	8	53	47%	**34%**
			CONFROOM_TOP_1	189	5	6	49%	1	1	9%	3	10	19%	9	50	44%	**30%**
			CONFROOM_TOP_2	126	5	6	47%	1	1	6%	3	8	17%	9	48	43%	**28%**
			OPENOFFICE_MID_4	194	5	6	49%	0	0	2%	3	7	14%	9	50	44%	**27%**
			ENCLOSEDOFFICE_BOT_3	126	5	6	52%	0	0	1%	3	5	11%	9	49	44%	**27%**
			ENCLOSEDOFFICE_BOT_4	126	5	6	51%	0	0	1%	3	5	10%	9	49	44%	**27%**
			CONFROOM_BOT_1	176	4	5	42%	0	0	3%	2	6	13%	9	45	40%	**24%**
			CONFROOM_MID_1	126	4	4	37%	0	1	4%	2	6	13%	8	40	36%	**22%**
			CONFROOM_BOT_2	126	4	4	38%	0	0	2%	2	6	11%	9	43	38%	**22%**
			CONFROOM_MID_2	126	3	4	31%	0	0	3%	2	6	11%	8	38	34%	**20%**
			OPENOFFICE_MID_1	43	4	5	40%	-	-	0%	3	4	7%	7	35	31%	**19%**
			OPENOFFICE_MID_2	43	4	5	40%	-	-	0%	3	4	7%	7	35	31%	**19%**
			OPENOFFICE_BOT_1	180	1	1	5%	-	-	0%	0	0	0%	6	16	15%	**5%**
			OPENOFFICE_BOT_2	45	1	1	5%	-	-	0%	0	0	0%	6	16	14%	**5%**

This makes indoor air easily heated and maintained during the hot days if there is no support of active air circulation from mechanical cooling and ventilation systems given power interruptions. Thus, we focus on hot thermal discomfort in the 2019 vintage office prototype. Table 9 provides a comprehensive analysis of the 2019 office's space-level thermal comfort over a 15-day period of power interruptions during a heatwave in 2054. The table includes

Table 8 Building scale cold discomfort rating from area-weighted average from the space-level integrated cold rating for the pre-1980 vintage office with EEMs during the 2023 extreme cold snap with power outage

Vintage	Scenario	EEM	Area-weighted average integrated cold rating	Effect
Pre1980	2023 cold snap	Baseline	52%	—
		Infiltration	36%	16% Improvement
		Thermal window	40%	12% Improvement
		Cool envelope	55%	3% Deterioration
		Solar-control window	70%	18% Deterioration

Table 9 Hot thermal discomfort rating for each workable space for 2019 code-compliant office during the 2054 heatwave with power outage

Vintage	Scenario	EEM	Space	Area [m²]	PMV>2 hours [h/d]	PMV>2 weighted discomfort hours [TSSU·h/d]	PMV hot rating	SET>30 hot stress hours [h/d]	SET>30 weighted hot stress hours [°C·h/d]	SET hot rating	Adaptive hot hours [h/d]	Adaptive weighted hot hours [°C·h/d]	Adaptive hot rating	HI caution hours [h/d]	HI caution weighted hours [°C·h/d]	HI caution rating	**Integrated hot rating**
2019	2054 Heatwave	Baseline	CONFROOM_TOP_2	43	10	13	100%	10	116	100%	10	43	100%	10	422	100%	**100%**
			CONFROOM_MID_2	43	10	13	100%	10	113	98%	10	39	90%	10	408	97%	**96%**
			CONFROOM_TOP_1	43	10	13	98%	10	110	95%	9	39	91%	10	398	94%	**95%**
			CONFROOM_MID_1	43	10	13	97%	10	108	93%	9	35	81%	10	387	92%	**91%**
			CONFROOM_BOT_2	43	10	13	98%	10	108	93%	9	30	70%	10	378	90%	**88%**
			CONFROOM_BOT_1	43	10	12	95%	10	102	88%	9	26	61%	10	356	84%	**82%**
			ENCLOSEDOFFICE_TOP_2	126	9	12	91%	9	41	35%	9	34	79%	10	109	26%	**58%**
			OPENOFFICE_TOP_1	194	7	9	72%	9	77	66%	6	11	25%	9	258	61%	**56%**
			OPENOFFICE_TOP_2	212	7	9	72%	9	77	66%	6	11	25%	9	258	61%	**56%**
			ENCLOSEDOFFICE_MID_2	126	9	11	88%	9	40	34%	9	30	68%	10	109	26%	**54%**
			OPENOFFICE_TOP_4	180	8	11	82%	9	41	36%	8	28	65%	10	117	28%	**53%**
			CLASSROOM_BOT	30	7	9	71%	10	69	60%	6	7	16%	10	234	56%	**51%**
			OPENOFFICE_MID_1	194	7	8	65%	9	69	60%	5	8	18%	9	228	54%	**49%**
			OPENOFFICE_MID_2	212	7	8	65%	9	69	60%	5	8	18%	9	228	54%	**49%**
			ENCLOSEDOFFICE_TOP_1	126	8	11	81%	9	34	29%	8	27	63%	10	95	22%	**49%**
			OPENOFFICE_MID_4	180	8	10	78%	9	41	35%	8	24	55%	10	119	28%	**49%**
			ENCLOSEDOFFICE_BOT_2	126	8	10	78%	9	40	34%	8	21	49%	10	117	28%	**47%**
			ENCLOSEDOFFICE_MID_1	126	8	10	77%	9	32	28%	8	23	54%	10	94	22%	**45%**
			ENCLOSEDOFFICE_BOT_4	45	8	9	73%	9	39	34%	7	15	34%	10	122	29%	**42%**
			ENCLOSEDOFFICE_BOT_3	45	8	9	73%	9	39	34%	7	14	33%	10	121	29%	**42%**
			ENCLOSEDOFFICE_BOT_1	126	7	9	72%	8	31	27%	7	15	34%	10	98	23%	**39%**
			OPENOFFICE_TOP_3	176	7	9	70%	8	30	26%	7	15	35%	10	92	22%	**38%**
			ENCLOSEDOFFICE_TOP_3	42	7	9	70%	8	28	24%	7	16	36%	10	86	20%	**38%**
			OPENOFFICE_BOT_2	212	5	7	51%	8	55	47%	3	3	7%	9	174	41%	**37%**
			OPENOFFICE_BOT_1	194	5	7	51%	8	53	46%	3	2	6%	9	168	40%	**36%**
			OPENOFFICE_MID_3	176	7	8	65%	7	29	25%	6	12	27%	10	92	22%	**35%**
			ENCLOSEDOFFICE_MID_3	42	7	8	65%	7	27	23%	6	12	28%	10	86	20%	**34%**
			OPENOFFICE_BOT_3	189	5	7	50%	7	27	23%	4	4	8%	9	93	22%	**26%**

the total number of hours, normalized by the heatwave duration, and weighted discomfort hours for each hot thermal comfort metric PMV, SET, adaptive model, and heat index for the ten hours of the daytime working hours.

All the hot thermal comfort metrics indicate that conference rooms in all floors experience at least nine hours of thermally hot conditions without any support of a mechanical cooling system. The study assumes the number of occupants is kept the same from the normal operating conditions as specified in the prototype model, which shows that the occupancy density in the conference room is higher than the other working spaces. The occupancy density for conference rooms is 0.6 person/m², while the occupancy density for office spaces is 0.06 person/m², and this brings more internal heat gain to the space causing more hot-related thermal uncomfortable conditions. Table 9 also provides a hot thermal performance rating for each space based on the weighted discomfort hours for each metric. The far-right column presents an integrated hot rating derived from Equation (2). This integrated metric indicates that the conference rooms are the most vulnerable to hot thermal discomfort. The offices on the top and middle floors located in the west and center are the next vulnerable space group. Spaces in the north and on the bottom floor are less vulnerable. Figure 6 illustrates the color-coded hot thermal discomfort rating in the top, mid, and bottom floor plans for the 2019 vintage office building under the power-interrupted extreme heatwave event in 2054 weather conditions.

3.3.2 *Hot thermal comfort improvement with passive EEMs*

Table 10 provides hot thermal comfort changes resulting from the application of solar-controlled window coatings. Window coating reduces solar heat gain by lowering the SHGC to 0.15 from the baseline condition. This measure mitigates the weighted hot discomfort by at least 36% for conference rooms and by at least 19% for other office spaces. Greater improvements are observed in the South, East, and

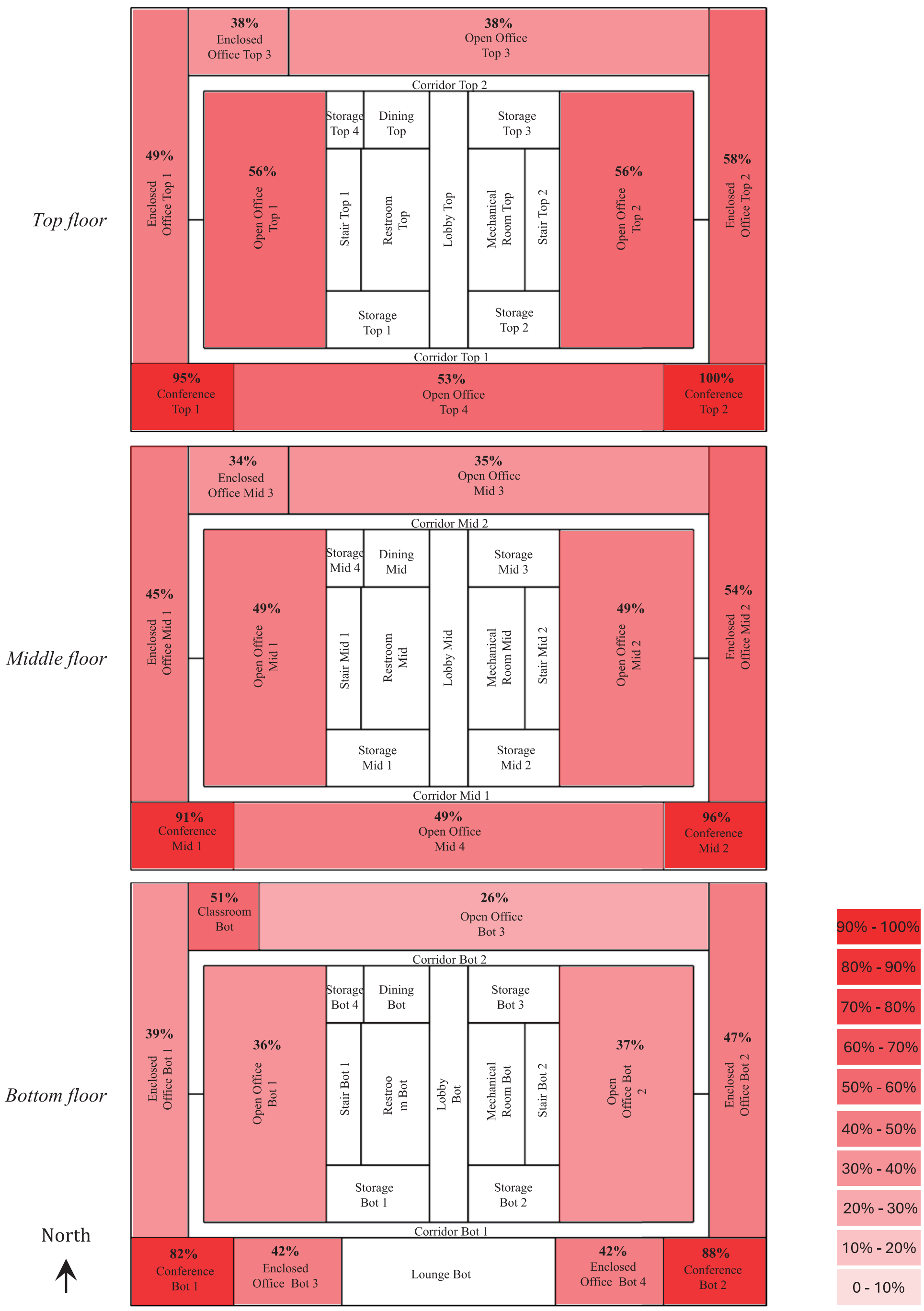

Fig. 6 Color-coded hot thermal discomfort rating in the top, middle, and bottom floor plans for the 2019 office building under power-interrupted extreme heatwave event in 2054

West perimeter spaces with windows, achieving at least a 31% reduction, while spaces located in the core zones and North perimeter see improvements of about 20%. Although the measure decreases the degree of hot discomfort, the heat index and SET metrics indicate that conference rooms remain in a discomfort condition for all hours, and most office spaces on the top and middle floors face discomfort conditions for most of the working hours. Among the four hot discomfort metrics, the adaptive weighted hot hours show the most improvement from window coatings.

Table 11 details the thermal comfort changes resulting from the cool envelope strategy, which involves bright-white painting that increases the solar reflectance to 0.6. The discomfort-weighted hour ratings show an improvement of 2% to 8%, depending on the location of the space, calculated based on the baseline worst space condition. Spaces on the

Table 10 Hot thermal discomfort rating for each workable space for the 2019 vintage office with solar-control window measure during the 2054 heatwave with power outage

Vintage	Scenario	EEM	Space	Area [m²]	PMV>2 hours [h/d]	PMV>2 weighted discomfort hours [TSSU·h/d]	PMV hot rating	SET>30 hot stress hours [h/d]	SET>30 weighted hot stress hours [°C·h/d]	SET hot rating	Adaptive hot hours [h/d]	Adaptive weighted hot hours [°C·h/d]	Adaptive hot rating	HI caution hours [h/d]	HI caution weighted hours [°C·h/d]	HI caution rating	**Integrated hot rating**
2019	2054 Heatwave	Solar-control Window	CONFROOM_TOP_2	43	9	12	90%	10	79	68%	7	11	25%	10	266	63%	**62%**
			CONFROOM_TOP_1	43	9	11	85%	10	76	66%	7	10	23%	10	258	61%	**59%**
			CONFROOM_MID_2	43	9	11	82%	10	75	64%	6	7	17%	10	250	59%	**56%**
			CONFROOM_MID_1	43	8	10	79%	10	72	62%	6	6	15%	10	242	57%	**53%**
			CONFROOM_BOT_2	43	7	9	66%	10	67	57%	4	2	5%	10	220	52%	**45%**
			CONFROOM_BOT_1	43	7	8	64%	10	63	55%	3	2	4%	10	211	50%	**43%**
			OPENOFFICE_TOP_1	194	6	7	53%	8	52	45%	-	-	0%	9	158	37%	**34%**
			OPENOFFICE_TOP_2	212	6	7	53%	8	52	45%	-	-	0%	9	158	37%	**34%**
			OPENOFFICE_MID_1	194	5	5	41%	8	42	36%	-	-	0%	9	126	30%	**27%**
			OPENOFFICE_MID_2	212	5	5	41%	8	42	36%	-	-	0%	9	126	30%	**27%**
			CLASSROOM_BOT	30	4	5	38%	8	41	36%	-	-	0%	10	139	33%	**27%**
			ENCLOSEDOFFICE_TOP_2	126	6	7	57%	8	14	12%	6	4	10%	10	60	14%	**24%**
			OPENOFFICE_TOP_4	180	6	6	50%	7	17	14%	4	3	7%	10	68	16%	**22%**
			ENCLOSEDOFFICE_TOP_1	126	5	6	43%	6	11	10%	4	3	7%	10	54	13%	**18%**
			OPENOFFICE_BOT_2	212	3	3	22%	7	31	27%	-	-	0%	8	96	23%	**18%**
			ENCLOSEDOFFICE_MID_2	126	5	5	41%	7	11	10%	2	2	4%	10	56	13%	**17%**
			OPENOFFICE_MID_4	180	4	5	35%	6	15	13%	2	1	3%	10	65	15%	**17%**
			OPENOFFICE_BOT_1	194	2	2	18%	7	29	25%	-	-	0%	8	90	21%	**16%**
			ENCLOSEDOFFICE_MID_1	126	3	4	30%	5	9	8%	2	1	3%	10	50	12%	**13%**
			OPENOFFICE_TOP_3	176	3	4	29%	6	11	9%	1	0	0%	9	55	13%	**13%**
			ENCLOSEDOFFICE_TOP_3	42	3	4	28%	6	9	8%	1	0	0%	9	51	12%	**12%**
			ENCLOSEDOFFICE_BOT_4	45	2	2	18%	6	13	11%	0	0	0%	9	62	15%	**11%**
			ENCLOSEDOFFICE_BOT_3	45	2	2	17%	6	13	11%	-	-	0%	9	61	15%	**11%**
			OPENOFFICE_MID_3	176	2	2	19%	5	9	8%	-	-	0%	9	51	12%	**10%**
			ENCLOSEDOFFICE_BOT_2	126	2	2	17%	6	9	8%	0	0	0%	9	53	12%	**9%**
			ENCLOSEDOFFICE_MID_3	42	2	2	16%	4	7	6%	-	-	0%	9	46	11%	**8%**
			ENCLOSEDOFFICE_BOT_1	126	1	1	9%	4	7	6%	0	0	0%	9	46	11%	**7%**
			OPENOFFICE_BOT_3	189	0	0	4%	4	8	7%	-	-	0%	9	45	11%	**5%**

Table 11 Hot thermal discomfort rating for each workable space for the 2019 vintage office with cool envelope measure during the 2054 heatwave with power outage

Vintage	Scenario	EEM	Space	Area [m²]	PMV>2 hours [h/d]	PMV>2 weighted discomfort hours [TSSU·h/d]	PMV hot rating	SET>30 hot stress hours [h/d]	SET>30 weighted hot stress hours [°C·h/d]	SET hot rating	Adaptive hot hours [h/d]	Adaptive weighted hot hours [°C·h/d]	Adaptive hot rating	HI caution hours [h/d]	HI caution weighted hours [°C·h/d]	HI caution rating	**Integrated hot rating**
2019	2054 Heatwave	Cool Envelope	CONFROOM_TOP_2	43	10	13	100%	10	109	95%	10	37	86%	10	390	92%	**93%**
			CONFROOM_MID_2	43	10	13	100%	10	109	95%	10	36	82%	10	390	92%	**92%**
			CONFROOM_TOP_1	43	10	13	97%	10	104	90%	9	34	77%	10	370	88%	**88%**
			CONFROOM_MID_1	43	10	13	97%	10	104	90%	9	32	74%	10	370	88%	**87%**
			CONFROOM_BOT_2	43	10	13	97%	10	105	91%	9	28	65%	10	366	87%	**85%**
			CONFROOM_BOT_1	43	10	12	94%	10	99	86%	8	24	56%	10	345	82%	**79%**
			ENCLOSEDOFFICE_TOP_2	126	9	11	86%	9	36	31%	9	28	64%	10	100	24%	**51%**
			ENCLOSEDOFFICE_MID_2	126	9	11	85%	9	37	32%	8	26	60%	10	104	25%	**50%**
			CLASSROOM_BOT	30	7	9	71%	10	67	58%	6	6	13%	10	226	54%	**49%**
			OPENOFFICE_TOP_1	194	7	8	65%	9	68	59%	5	6	15%	9	222	53%	**48%**
			OPENOFFICE_TOP_2	212	7	8	65%	9	68	59%	5	6	15%	9	222	53%	**48%**
			OPENOFFICE_TOP_4	180	8	10	80%	9	36	31%	8	22	51%	10	106	25%	**47%**
			OPENOFFICE_MID_1	194	7	8	64%	9	65	56%	5	6	13%	9	211	50%	**46%**
			OPENOFFICE_MID_2	212	7	8	64%	9	65	56%	5	6	13%	9	211	50%	**46%**
			OPENOFFICE_MID_4	180	8	10	76%	9	38	33%	7	20	47%	10	113	27%	**46%**
			ENCLOSEDOFFICE_BOT_2	126	8	10	77%	9	38	32%	8	19	43%	10	112	27%	**45%**
			ENCLOSEDOFFICE_TOP_1	126	8	10	77%	9	29	25%	8	22	50%	10	86	20%	**43%**
			ENCLOSEDOFFICE_MID_1	126	8	10	75%	9	30	26%	7	20	47%	10	89	21%	**42%**
			ENCLOSEDOFFICE_BOT_4	45	8	9	72%	9	37	32%	7	13	30%	10	117	28%	**41%**
			ENCLOSEDOFFICE_BOT_3	45	7	9	72%	9	37	32%	7	12	29%	10	116	28%	**40%**
			ENCLOSEDOFFICE_BOT_1	126	7	9	70%	8	30	26%	7	13	30%	10	95	22%	**37%**
			OPENOFFICE_BOT_2	212	5	7	51%	8	52	45%	3	2	5%	9	165	39%	**35%**
			OPENOFFICE_BOT_1	194	5	7	50%	8	50	44%	3	2	4%	9	159	38%	**34%**
			OPENOFFICE_TOP_3	176	7	8	64%	7	25	21%	6	10	24%	10	82	19%	**32%**
			ENCLOSEDOFFICE_TOP_3	42	7	8	64%	7	23	20%	6	11	25%	10	77	18%	**32%**
			OPENOFFICE_MID_3	176	7	8	63%	7	26	22%	6	9	21%	10	87	21%	**32%**
			ENCLOSEDOFFICE_MID_3	42	7	8	62%	7	24	21%	6	10	22%	10	81	19%	**31%**
			OPENOFFICE_BOT_3	189	5	6	47%	7	25	22%	4	2	5%	9	89	21%	**24%**

top floor benefit the most from the cool roof application. Although the cool envelope strategy helps mitigate some hot discomfort, most of the working spaces still face discomfort conditions for most of the working hours, indicating limited effectiveness in decreasing the overall discomfort hours.

Table 12 presents the building-level hot thermal performance rating changes resulting from the aforementioned EEMs. This building-level rating was derived by integrating space-level ratings using an area-weighted average. The baseline condition shows a discomfort rating of 44%.

Table 12 Building scale hot discomfort rating from area-weighted average from the space-level integrated hot rating for the 2019 vintage office with EEMs during the 2054 extreme heatwave with power outage

Vintage	Scenario	EEM	Area-weighted average integrated hot rating	Effect
2019	2054 heatwave	Baseline	44%	—
		Solar-control window	10%	34% Improvement
		Cool envelope	36%	8% Improvement
		Infiltration	48%	4% Deterioration

Implementing the window coating measure reduces the building-level weighted discomfort to 10%, representing a 34% improvement. The cool envelope strategy contributes an 8% improvement at the building scale. Conversely, the infiltration measure has a negative effect during the heatwave period, worsening the discomfort rating by 4%. Note that the 2019 vintage office building already features low U-value window systems, so no thermal window measure was implemented in this heatwave thermal comfort analysis.

3.4 Discussions

3.4.1 *Extreme climate scenarios*

This study presents an approach to understanding and projecting the impacts of future climate using Future Typical Meteorological Year (fTMY) weather data. The fTMY methodology, derived from the Typical Meteorological Year (TMY) approach, employs statistical techniques to select representative months from future climate model projections, thereby creating a single year of data that encapsulates expected climatic conditions. This method leverages scenarios provided by the IPCC, specifically utilizing the SSP5-RCP8.5 scenario. The resulting fTMY data is used in building simulations to assess the impact of future climate scenarios on the changes in building energy performance.

The study also focuses on the detection and analysis of extreme climate events, such as heatwaves and cold snaps, using an hourly future weather dataset derived from regional climate models. By employing a method based on high and low quantiles of daily air temperature distribution, the study effectively identifies and characterizes heatwave and cold snap extreme events. This method is advantageous as it uses relative thresholds, making it applicable across various global locations. This approach has proven effective for building resilience analysis, highlighting its utility in evaluating the thermal comfort and safety for occupants and thermal resilience of buildings to future climate events. The findings indicate a substantial increase in the frequency and severity of extreme heat events over time, whereas future cold extremes are projected to be less pronounced compared to current climate conditions. Notably, the most severe cold snap was detected in 2023, within the ten-year period from 2014 to 2023. However, as global temperatures rise, future cold snaps were not observed in the data projected for 2045 to 2054, based on the same temperature threshold of the recent decade. Conversely, future heatwaves are projected to increase in both duration and severity. For instance, the most intense event in 2054 lasted three times longer and reached daily mean temperatures nearly 7 °C higher than recent events. This study focused on identifying and analyzing the most severe climate events under the given location and climate scenarios. While other cold snap and heatwave events of lesser severity were also present, the objective was to screen and evaluate the most extreme cases. The primary aim was to assess thermal discomfort under power outage conditions during these peak climate stress events.

Simulation results show that during such events, even ASHRAE 90.1–2019-compliant buildings—typically viewed as resilient—experienced significant thermal discomfort under power outage conditions, especially in top-floor perimeter zones. These findings emphasize that modern building performance can degrade during grid failures, particularly in airtight buildings without passive cooling strategies. They also reinforce the importance of integrating passive energy efficiency measures—such as infiltration control and solar-controlled windows—which in our simulations reduced thermal discomfort by up to 21% during cold snaps and 34% during heatwaves. Thus, building resilience planning must not only consider average climate trends but also explicitly prepare for infrequent but high-impact extreme events, especially under conditions where active HVAC systems are unavailable.

3.4.2 *Realistic building models for simulation-based performance analysis*

We used the prototype medium office building energy models representing pre-1980 vintage and ASHRAE 90.1-2019 compliant office buildings. The study focused on two building vintages: the poorest-performing and the most recent code-compliant design. While additional vintages could have been included to examine how incremental improvements in building envelopes and energy systems respond to climate change and extreme events, we prioritized understanding the performance of these two extremes. The model has various space types in three floors including open office and enclosed office spaces and conference rooms, which reflects a more realistic thermal zoning office building. This enabled the analysis of occupants' intra-building thermal comfort in the context of evaluating thermal comfort key performance indicators for different space types across various locations and floors. Intra-building space-level analysis can analyze targeted opportunities that strategize at the space- or room-level. Still there are limitations to using normative occupants density and schedule under the extreme events with power outage for thermal comfort analysis. Reflecting realistic working conditions such as activities and schedules for occupants who conduct mission-critical tasks under power outage conditions or a dynamic occupancy scenario, incorporating behavioral adaptations informed by the present findings can be applied in a case study of resilience-mode occupancy. Future research should investigate how occupant relocation to less uncomfortable spaces during extreme events influences thermal comfort ratings, as such analysis could yield additional insights into adaptive strategies. This would allow thermal habitability evaluation at the space level and then link these spaces with work-critical assets that require thermal habitability to assure operations.

The ASHRAE 90.1-2019 code-compliant building incorporates advanced energy-efficient technologies, resulting in significantly lower energy consumption compared to the pre-1980 model. Specifically, the 2019 model shows a 37% reduction in electricity consumption and a 49% reduction in natural gas consumption, attributed to efficient HVAC systems, lighting, electric equipment, and improved thermal insulation.

While the energy performance advantages of high-efficiency envelopes and HVAC systems are well documented in the literature, we present these results to establish a baseline understanding of the trade-offs between energy efficiency and thermal resilience under climate stress. Our intent is not to repeat general findings, but to show how these differences in vintage performance affect indoor thermal safety during outages—a situation not typically captured in conventional energy studies.

The prototype employs a natural gas-based central boiler and an electric terminal reheat system for heating. Under 2020 fTMY weather conditions, the pre-1980 building's heating source energy is 6.4 times greater than its cooling source energy, changing to 3.9 times under 2050 conditions due to future climate. The 2019 building shows a heating source energy consumption 2.8 times higher than cooling in 2020, changing to 1.7 times in 2050. Projected climate in 2050 increases cooling energy consumption by 33% and decreases heating energy consumption by 19% for the 2019 building. Passive thermal resilient technologies, such as improved airtightness and low-U-value thermal windows, can reduce heating energy by approximately 12% in pre-1980 buildings and 4% in 2019 buildings. Solar-control window films can reduce cooling energy consumption by 20% in the 2019 office and 15% in the pre-1980 office. Cool envelope strategies contribute to an additional 3% savings in cooling energy. These measures slightly increase electric reheat energy but reduce natural gas heating energy, leading to minor changes in overall heating source energy performance. This study does not aim to rank individual measures or assess the combined effects of retrofit packages. Parametric simulations involving varying levels and combinations of passive strategies could yield more statistically significant insights into mitigation potential.

These findings are crucial because they demonstrate that passive EEMs—which are often adopted for their efficiency benefits—can also enhance or at least preserve thermal resilience under climate extremes. By presenting these results, we quantify the baseline energy shifts that underpin the building's capacity to maintain safe conditions when active systems fail, helping bridge the gap between energy performance and resilience planning.

3.4.3 *Thermal comfort mitigation*

The utilization of multiple thermal comfort metrics provides a comprehensive evaluation of occupant comfort under extreme climate conditions. The PMV–PPD, SET, adaptive model, hours of safety, and heat index metrics each offer unique insights into different aspects of thermal comfort. The study focused on 28 office-related spaces during working hours (8 a.m. to 6 p.m.). Weighted discomfort hours were calculated for recent (2023) and future (2054) extreme cold snap and heatwave climate events, assuming power outages to assess thermal comfort without HVAC support. The results were normalized to compare outcomes across varying durations of cold snaps and heatwaves. This approach not only captures the diversity of occupant thermal responses but also allows us to identify specific spaces that are most vulnerable under climate stress. By integrating these metrics, the study effectively assesses the thermal comfort and safety of office buildings and the potential impact of future climate scenarios on occupant comfort. The findings inform space-level risk analysis and support the development of targeted resilience strategies, such as passive retrofit prioritization or occupant relocation during outages. This holistic approach is essential for developing strategies to enhance building performance and ensure occupant well-being in the face of future climate.

Thermal habitability in buildings can be improved by retrofitting buildings to meet the latest commercial building energy codes, such as ASHRAE 90.1-2019. This intervention would significantly increase the building envelope insulation, reduce the amount of infiltration, and would provide a longer thermal habitability timeframe in case of a power outage in cold snap events. Passive measures such as improved thermal windows, envelope insulation and less infiltration airflow can achieve thermal comfort in the cold season. In our simulation, these strategies led to up to a 21% reduction in cold discomfort hours, particularly in top-floor perimeter zones, which were found to be the most vulnerable. If power outages are anticipated under any circumstances during the cold season, fuel or electric battery-powered portable heaters can be used for heating targeted areas for mission-critical spaces. This portable heating equipment can keep the indoor environment in thermally habitable conditions during power and steam outage events. These approaches, though well-known, become critical when centralized heating fails and localized thermal safety becomes the primary concern, especially for facilities where relocation is not feasible. In addition, preheating building spaces above the heating setpoint temperature can contribute to prolonging the indoor environment to thermally habitable conditions. The preheated air temperature will keep the indoor environment thermally habitable for a longer duration depending on the building structure thermal inertia compared to keeping the indoor air temperature with the normal setpoint temperature (Christensen et al. 2022). This strategy, while common, was not simulated directly in this study but is consistent with the role of thermal mass observed in the space-level discomfort patterns.

The pre-1980 vintage office building is significantly more vulnerable to cold thermal discomfort during cold snap events compared to the 2019 office building. The integrated cold discomfort rating indicates that the top floor offices located in the north are the most vulnerable to cold thermal discomfort. Perimeter zones on the top and bottom floors are particularly susceptible, with the top floor performing the worst. South-facing offices and inner zones without windows are safer during cold events. Conference and classroom spaces with higher occupant densities offer better protection during cold snaps. Our results can inform occupant location strategies to improve thermal safety after power interruptions during extreme cold snap weather events when evacuation is not possible or reasonable. We find that reallocating occupants from top floor north perimeter spaces to bottom floor central spaces within building can improve the cold thermal discomfort conditions by 92% in pre-1980 vintage office buildings (Figure 5). Passive energy efficiency measures, such as reducing infiltration and upgrading windows with low U-value, significantly improve cold thermal comfort. Personal factors such as clothing insulation level and metabolic rate from activity conditions affect thermal habitability. Although our analysis assumes fixed occupant clothing and activity levels, prior research shows that individuals with higher insulation clothing or metabolic activity can tolerate colder indoor conditions. These personal factors could be considered in future studies to refine estimates of thermal habitability.

An interesting result is that the 2019 vintage office building may face more dangerous indoor thermal conditions during severe heatwave climate events. The recent building code, which emphasizes airtightness and thermal insulation, can lead to higher indoor temperatures during hot days without mechanical cooling. The hot discomfort rating indicates that conference rooms are the most vulnerable to hot thermal discomfort. During the 2054 heatwave event, the average SET in conference rooms exceeded 31.5 °C, and PMV values often exceeded +2.5 for several consecutive hours. The higher occupancy density in conference rooms compared to other office spaces results in more internal heat gain, causing more hot-related discomfort. Other office spaces on the top and middle floors located in the south, west, east and center zones are more vulnerable than other spaces in the north and on the bottom floor. For example, center-south zones on the top floor recorded the highest hourly heat index values, reaching 37.8 °C, and exceeded the ASHRAE comfort range for more than 60% of occupied hours during the outage period. Our findings show occupant location strategies to improve thermal safety after power interruptions during extreme heatwave events when evacuation is not an option. We find that reallocating occupants from top floor central office spaces to bottom floor north spaces within the building can improve the hot thermal discomfort conditions by 30% in 2019 vintage office buildings under the 2050 weather condition (Figure 6). Solar-control window coatings and cool envelope strategies help mitigate hot discomfort. In our simulation, applying solar-control films alone reduced hot discomfort hours by up to 34% in the most vulnerable spaces, particularly in south-facing zones. Also, the natural ventilation opening windows can be considered depending on the outdoor air temperature and wind speed conditions. Although natural ventilation was not explicitly modeled, it may offer additional cooling potential if outdoor conditions are favorable.

4 Conclusions

This study underscores the critical importance of enhancing the thermal resilience of office buildings in the face of escalating extreme climate events, characterized by increasingly severe heatwaves and cold snaps. Utilizing a detailed medium office building energy model, representative of both pre-1980 and ASHRAE 90.1-2019 compliant structures, the research provides valuable insights into the effectiveness of passive EEMs in improving thermal comfort and reducing energy consumption under extreme weather conditions.

The findings indicate that future climate will significantly impact building energy performance, with a projected increase in cooling energy demand and a decrease in heating energy consumption. The 2019 vintage office building, compliant with the recent energy codes, demonstrates substantial energy savings compared to the pre-1980 model, attributed to advanced HVAC systems, energy efficient lighting, and improved thermal insulation. However, this recent vintage building is also more vulnerable to indoor thermal discomfort during heatwaves due to its airtight and well-insulated design, which can trap heat without active cooling. Passive EEMs such as infiltration control, thermal windows, cool envelopes, and window coatings were evaluated for their effectiveness in mitigating thermal discomfort during extreme climate events. Infiltration control and thermal window upgrades significantly improved cold thermal comfort in pre-1980 buildings, highlighting the importance of reducing unwanted airflow and enhancing thermal insulation. On the other hand, solar-control window films and cool envelope strategies were more effective in reducing heat gain and improving thermal comfort during heatwaves, particularly in the 2019 vintage office building.

The comprehensive approach, incorporating multiple thermal comfort metrics like PMV–PPD, SET, adaptive model, hours of safety, and heat index, provides a robust framework for assessing occupant comfort under varying climate scenarios. The results emphasize the need for targeted occupancy allocation strategies that consider space or floor-level vulnerabilities to enhance thermal resilience. This study underscores the importance of passive energy efficiency measures in improving thermal comfort, particularly for a power outage under extreme weather conditions. By addressing key aspects such as infiltration control, window insulation, and solar reflectance, these measures contribute to mitigating the thermal discomforts. The insights gained from this research are expected to inform future building design and retrofitting practices, promoting the development of resilient built environments capable of withstanding the challenges posed by future climate scenarios.

Acknowledgements

The authors would like to acknowledge the U.S. Department of Energy Office of Electricity and the Office of Energy Efficiency and Renewable Energy for funding on the Energy Resilience for Mission Assurance (ERMA) project. This work was supported by the Assistant Secretary for Energy Efficiency and Renewable Energy, Building Technologies Office, of the U.S. Department of Energy under Contract No. DE-AC02-05CH11231. This work was authored in part by the National Renewable Energy Laboratory for the U.S. Department of Energy (DOE) under Contract No. DE-AC36-08GO28308. The views expressed in the article do not necessarily represent the views of the DOE or the U.S. Government. The U.S. Government retains and the publisher, by accepting the article for publication, acknowledges that the U.S. Government retains a nonexclusive, paid-up, irrevocable, worldwide license to publish or reproduce the published form of this work, or allow others to do so, for U.S. Government purposes.

Declaration of competing interest

The authors have no competing interests to declare that are relevant to the content of this article.

Ethics approval

This study does not contain any studies with human or animal subjects performed by any of the authors.

Author contribution statement

All authors contributed to the study conception and design. Sang Hoon Lee led the methodology development and simulation analysis. Carlo Bianchi contributed to modeling and weather dataset development. Juan Pablo Carvallo supported manuscript editing and securing funding. All authors contributed to the writing and reviewed and approved the final manuscript.

References

Al-Assaad D, Sengupta A, An P, et al. (2025). Resilient passive cooling strategies during heat waves: A quantitative assessment in different climates. *Building and Environment*, 274: 112698.

ASHRAE (2017). ANSI/ASHRAE Standard 55-2017: Thermal Environmental Conditions for Human Occupancy. Atlanta, GA, USA: American Society of Heating, Refrigerating and Air-Conditioning Engineers.

ASHRAE (2020). ANSI/ASHRAE Addendum a to ANSI/ASHRAE Standard 169-2013: Climatic Data for Building Design Standards.

Attia S, Levinson R, Ndongo E, et al. (2021). Resilient cooling of buildings to protect against heat waves and power outages: Key concepts and definition. *Energy and Buildings*, 239: 110869.

Ayyagari S, Gartman M, Corvidae J (2020). A Framework for Considering Resilience in Building Envelope Design and Construction. Rocky Mountain Institute, USA.

Chowdhury S, Li F, Avery S, et al. (2024). Future Typical Meteorological Year (fTMY) US Weather Files for Building Simulation for every US County in CONUS (Cross-Model Version-SSP5-RCP8.5). Available at https://zenodo.org/records/10672440. Accessed 8 Aug 2025.

Christensen LRL, Broholt TH, Barthelmes VM, et al. (2022). A mixed-methods case study on resident thermal comfort and attitude towards peak shifting of space heating. *Energy and Buildings*, 276: 112501.

DOE (2023). EnergyPlus™ Version 23.1.0 Documentation Input Output Reference. U.S. Department of Energy.

Doss-Gollin J, Farnham DJ, Lall U, et al. (2021). How unprecedented was the February 2021 Texas cold snap? *Environmental Research Letters*, 16: 064056.

Erba S, Barbieri A (2022). Retrofitting buildings into thermal batteries for demand-side flexibility and thermal safety during power outages in winter. *Energies*, 15: 4405.

Field CB, Barros V, Stocker TF, et al. (2012). Managing the Risks of Extreme Events and Disasters to Advance Climate Change Adaptation: Special Report of the Intergovernmental Panel on Climate Change. Cambridge, UK: Cambridge University Press.

Flores-Larsen S, Bre F, Hongn M (2022). A performance-based method to detect and characterize heatwaves for building resilience analysis. *Renewable and Sustainable Energy Reviews*, 167: 112795.

Gelaro R, McCarty W, Suárez MJ, et al. (2017). The modern-era retrospective analysis for research and applications, version 2 (MERRA-2). *Journal of Climate*, 30: 5419–5454.

Goel S, Athalye R, Wang W, et al. (2014). Enhancements to ASHRAE Standard 90.1 Prototype Building Models. Pacific Northwest National Laboratory.

Green-Mignacca S, Rostami M, Bucking S (2024). Towards codification of thermal resilience upgrades in midrise residential buildings: A Canadian archetype energy model approach. *Journal of Building Performance Simulation*, https://doi.org/10.1080/19401493.2024.2435908.

GTI Energy (2023). Source energy and emissions analysis tool commercial buildings. Available at https://cmicseeatcalc.gti.energy/CommercialBuildings

Hachem-Vermette C, Yadav S (2023). Impact of power interruption on buildings and neighborhoods and potential technical and design adaptation methods. *Sustainability*, 15: 15299.

Hinge A (2023). Resilience Issues in Building Energy Codes. IEA EBC Building Energy Codes Working Group, International Energy Agency.

Holzer P, Stern P, Czarnecki P, et al. (2024). International Energy Agency - Resilient Cooling of Buildings - Technology Profiles Report (Annex 80). Institute of Building Research & Innovation.

Homaei S, Hamdy M (2021). Thermal resilient buildings: How to be quantified? A novel benchmarking framework and labelling metric. *Building and Environment*, 201: 108022.

Hong T, Lee SH, Zhang W, et al. (2023a). Nexus of electrification and energy efficiency retrofit of commercial buildings at the district scale. *Sustainable Cities and Society*, 95: 104608.

Hong T, Malik J, Krelling A, et al. (2023b). Ten questions concerning thermal resilience of buildings and occupants for climate adaptation. *Building and Environment*, 244: 110806.

IEA (2023). IEA EBC Annex 80 - Resilient Cooling of Buildings. Available at https://annex80.iea-ebc.org/

Im P, New JR, Bae Y (2019). Updated OpenStudio small and medium office prototype models. In: Proceedings of International IBPSA Building Simulation Conerence, Rome, Italy.

IPCC (2023). Sections. In: Climate Change 2023: Synthesis Report. Contribution of Working Groups I, II and III to the Sixth Assessment Report of the Intergovernmental Panel on Climate Change. Geneva: Intergovernmental Panel on Climate Change.

Ismail N, Ouahrani D, Al Touma A (2023). Quantifying thermal resilience of office buildings during power outages: Development of a simplified model metric and validation through experimentation. *Journal of Building Engineering*, 72: 106564.

ISO (2005). ISO 7730:2005: Ergonomics of the thermal environment - Analytical determination and interpretation of thermal comfort using calculation of the PMV and PPD indices and local thermal comfort criteria.

ISO (2017). ISO 17772-1:2017: Energy performance of buildings - Indoor environmental quality - Part 1: Indoor environmental input parameters for the design and assessment of energy performance of buildings.

ISO (2018). ISO/TR 17772-2:2018: Energy performance of buildings - Overall energy performance assessment procedures - Part 2: Guideline for using indoor environmental input parameters for the design and assessment of energy performance of buildings.

Kiersma ME (2014). Occupational safety and health administration. In: Wexler P (Eds), Encyclopedia of Toxicology. New York: Academic Press.

Lee K, Schiavon S (2014). Influence of three dynamic predictive clothing insulation models on building energy use, HVAC sizing and thermal comfort. *Energies*, 7: 1917–1934.

Lee SH, Levinson R (2023). Cool envelope benefits in future typical weather and heatwave conditions for single-family homes in Los Angeles. In: Proceedings of Sixth International Conference on Countermeasures to Urban Heat Islands, Melbourne, Australia.

Lee SH, Hong T, Le M, et al. (2024). Assessment of energy and thermal resilience performance to inform climate mitigation of multifamily buildings in disadvantaged communities. *Sustainable Cities and Society*, 104: 105319.

Liang J, Qiu YL, Wang B, et al. (2025). Impacts of heatwaves on electricity reliability: Evidence from power outage data in China. *iScience*, 28: 111855.

Machard A, Salvati A, Tootkaboni MP, et al. (2024). Typical and extreme weather datasets for studying the resilience of buildings to climate change and heatwaves. *Scientific Data*, 11: 531.

Mathew P, Sanchez L, Lee S, et al. (2021). Assessing the energy resilience of office buildings: Development and testing of a simplified metric for real estate stakeholders. *Buildings*, 11: 96.

NOAA National Centers for Environmental Information (2025). Global Hourly - Integrated Surface Database (ISD). Available at https://registry.opendata.aws/noaa-isd/. Accessed 18 Aug 2025.

NREL (2024). OpenStudio-Standards. Available at https://github.com/NREL/openstudio-standards. Accessed 25 Jul 2024.

Ouzeau G, Soubeyroux JM, Schneider M, et al. (2016). Heat waves analysis over France in present and future climate: Application of a new method on the EURO-CORDEX ensemble. *Climate Services*, 4: 1–12.

Samuelson HW, Baniassadi A, Gonzalez PI (2020). Beyond energy savings: Investigating the co-benefits of heat resilient architecture. *Energy*, 204: 117886.

Sheng M, Reiner M, Sun K, et al. (2023). Assessing thermal resilience of an assisted living facility during heat waves and cold snaps with power outages. *Building and Environment*, 230: 110001.

Siu CY, O'Brien W, Touchie M, et al. (2023). Evaluating thermal resilience of building designs using building performance simulation—A review of existing practices. *Building and Environment*, 234: 110124.

Siu CY, Touchie M, O'Brien W (2024). Development and testing of an automated tool to leverage building energy models for thermal resilience analysis. *Journal of Building Performance Simulation*, https://doi.org/10.1080/19401493.2024.2365381.

Steadman RG (1979). The assessment of sultriness. part I: A temperature-humidity index based on human physiology and clothing science. *Journal of Applied Meteorology*, 18: 861–873.

Stone B Jr, Mallen E, Rajput M, et al. (2021). Compound climate and infrastructure events: How electrical grid failure alters heat wave risk. *Environmental Science & Technology*, 55: 6957–6964.

USGBC (2024). Passive Survivability and Back-up Power During Disruptions. U.S. Green Building Council. Available at https://www.usgbc.org/credits/new-construction-core-and-shell-schools-new-construction-retail-new-construction-data-48?view=resources. Accessed 26 Sep 2024.

Vijayan DS, Sivasuriyan A, Patchamuthu P, et al. (2022). Thermal performance of energy-efficient buildings for sustainable development. *Environmental Science and Pollution Research*, 29: 51130–51142.

Villa DL, Schostek T, Bianchi C, et al. (2022). The Multi-scenario Extreme Weather Simulator. Sandia National Laboratories.

Villa DL, Lee SH, Bianchi C, et al. (2024). Multi-scenario Extreme Weather Simulator application to heat waves: Ko'olauloa community resilience hub. *Science and Technology for the Built Environment*, 30: 375–393.

Wagner A, O'Brien W, Dong B (2018). Exploring Occupant Behavior in Buildings. Cham, switzerland: Springer.

Wilcox S, Marion W (2008). Users Manual for TMY3 Data Sets. Golden, CO, USA: National Renewable Energy Laboratory (NREL).

Yoon N, Hoon Lee S, Arens E, et al. (2021). Assessing performance of passive or low-energy resilient cooling technologies for pre-1980 medium office buildings in Phoenix, Arizona and Chicago, Illinois. In: Proceedings of International IBPSA Building Simulation Conference.

Zeng Z, Kim J-H, Wang J, et al. (2023). Dynamically downscaled hourly future weather data with 12-km resolution covering most of North America. Argonne National Laboratory, USA.

Zhang C, Kazanci OB, Levinson R, et al. (2021). Resilient cooling strategies–A critical review and qualitative assessment. *Energy and Buildings*, 251: 111312.

Zhang C, Kazanci OB, Attia S, et al (2023). IEA EBC Annex 80 - Dynamic simulation guideline for the performance testing of resilient cooling strategies: Version 2.